NYO-9751

REACTION MECHANISMS IN LOW ENERGY INELASTIC PROTON SCATTERING

by

Hiroshi Taketani and W. Parker Alford

THE UNIVERSITY OF ROCHESTER

DEPARTMENT OF PHYSICS AND ASTRONOMY

ROCHESTER , NEW YORK

AEC DISTRIBUTION LIST

U. S. Atomic Energy Commission (2 copies)
New York Operations Office
Contracts Division
376 Hudson Street
New York 14, New York

U. S. Atomic Energy Commission (1 copy)
Division of Research
Washington 25, D. C.

U. S. Atomic Energy Commission (1 copy)
Brookhaven Area Office
NYO Patent Group
Upton, Long Island, New York

U. S. Atomic Energy Commission (3 copies)
Office of Technical Information Extension
P. O. Box 62
Oak Ridge, Tennessee

U. S. Atomic Energy Commission (1 copy)
Patents Group
Upton, New York
ATTENTION: Harmon Potter

U. S. Atomic Energy Commission (1 copy)
Washington 25, D. C.
ATTENTION: Roland Anderson

U. S. Atomic Energy Commission (1 copy)
Washington 25, D. C.
ATTENTION: Office of Technical Information

REPORT NUMBER NYO-9751

Reaction Mechanisms in Low Energy Inelastic Proton Scattering

by

Hiroshi Taketani* and W. Parker Alford

Department of Physics and Astronomy
University of Rochester
Rochester, New York

Contract Number (AT-(30-1)-875

August 21, 1961

* Now at the Department of Physics, University of Maryland, College Park, Maryland

ABSTRACT

A number of (pp') angular distributions and (p,p'γ) angular correlations have been measured in order to investigate the reaction mechanisms involved in inelastic proton scattering at low energies. Angular distributions were measured for the following nuclei at the energies (center of mass) indicated: A^{40} 6.14 Mev (first, second, and third excited states); Ni^{58} 4.70, 5.64, 6.65-6.80 Mev (first excited state); Ni^{60} 4.69, 5.63, 6.65-6.80 Mev (first excited state); Cu^{65} 6.83 Mev (second and third excited states). Angular correlations between protons leading to the first excited state and subsequent decay gamma rays were measured for the following nuclei: Si^{28}, 5.66, 6.70 Mev, $\theta_{p'} = 45^{\circ}, 90^{\circ}, 135^{\circ}$; S^{32} 5.66 Mev, $\theta_{p'} = 90^{\circ}, 135^{\circ}$; Ti^{48} 5.72, 6.77 Mev, $\theta_{p'} = 90^{\circ}, 135^{\circ}$; Ni^{58} 5.73, 6.80 Mev, $\theta_{p'} = 45^{\circ}, 90^{\circ}, 135^{\circ}$; Ni^{60} 5.73, 6.80 Mev, $\theta_{p'} = 50^{\circ}, 90^{\circ}, 135^{\circ}$.

For the odd-even nucleus Cu^{65}, the angular distributions show a prominent forward peaking, indicating the importance of a direct interaction mechanism at this energy. For the even-even nuclei in the neighborhood of A = 60, both angular distributions and correlations show agreement with the predictions of the statistical compound nucleus model for proton energies less than 6 Mev but indicate an appreciable direct interaction contribution at 7 Mev. Angular correlations for Si^{28} show that direct interactions are important in this case at both 5.66 and 6.70 Mev. It appears that the importance of direct interaction relative to compound nucleus contributions increases rapidly as the energy of the incident and emergent protons approaches the height of the Coulomb barrier, though it is clear that the structure of the nuclear states involved is also important in determining this ratio.

I. INTRODUCTION

One of two contrasting models is commonly used to describe the reaction mechamisms involved in the interaction of nucleons or light particles such as deuterons or alphas with nuclei. Processes proceeding through the formation of a compound nucleus (CN) are characterized by the formation of a relatively long-lived intermediate state in which the energy of the incident particle is shared with all the particles in the nucleus. The occurrence of discrete narrow resonances in scattering and reaction cross sections at low bombarding energies indicates the importance of CN processes under these conditions. At the other extreme is the direct interaction (DI) model in which the incident particle interacts with only a few degrees of freedom during the time that the incident particle takes to pass the nucleus.

The reaction mechanisms important in inelastic proton scattering at low energies have recently been studied by several workers [1-4] through measurements of the angular distributions of the inelastic protons and of the angular correlation between the inelastic protons and subsequent decay gamma rays. The results to be expected for CN processes depend upon the number of resonances excited in the compound state. For light nuclei at very low energies only a single resonance may be involved, in which case the angular distribution will generally change rapidly as the beam energy is varied over the resonance, but will always be symmetric about 90°. At somewhat higher energies, a few closely spaced resonances may be excited. In this case the angular distributions will still show rapid energy variations, but as a result of interference between different levels, will not generally show symmetry about 90°. At higher energies or for heavier nuclei, it may be possible to excite many resonances in the compound state. In this situation the statistical assumption[5] is usually made. Here it is assumed that the

signs of the reduced width amplitudes of the different levels are distributed randomly, so that angular distributions may be computed as averages over the many compound states, with the effects of interferences between different levels averaging to zero. The resultant angular distributions then show symmetry about 90° with only small deviations from isotropy and only slight variation with energy.

In a resonant reaction proceeding through a state of definite spin and parity in the compound nucleus, the angular correlation between inelastically scattered protons and subsequent gamma rays may be calculated using the results of Devons and Goldfarb[6]. The correlation depends upon the spins and parities of the states involved, and on the multipolarity of the gamma ray, so that no simple generalizations can be made about possible symmetries in the correlation function. It is clear however that if one or a few resonances are involved in the compound state, then the correlation function will be expected to vary rapidly with the energy of the incident particles, but if many levels are excited in the compound state, and the statistical assumption is valid, the correlation will not be sensitive to energy.

In the simplest direct interaction theory[7], the incident and emergent particles are represented as plane waves and the interaction with the nucleus is assumed to be of zero range and to take place at a definite radius R. The resultant angular distribution of the scattered particles is then proportional to $|J_L(qR)|^2$ where L and q are the angular and linear momentum transferred in the interaction. For the case of inelastic scattering from the 0^+ ground state to the 2+ first excited state of an even-even nucleus, L = 2, and the cross section should show a pronounced peaking the forward direction. If the Coulomb and nuclear distortion of the incident and outgoing waves is taken into account, and if the interaction is assumed to take place throughout

the nuclear volume, the resultant cross section may differ considerably from this simple result, but in general will show a marked asymmetry about 90°.

Satchler[8] has shown that for a $0^{+} \longrightarrow 2^{+} \longrightarrow 0^{+}$ transition the angular correlation between the inelastic proton and the subsequent gamma ray predicted by the simple plane wave DI theory is $W(\theta) = \sin^{2} 2(\theta_{\gamma} - \theta_{R})$ where θ_{γ} and θ_{R} are the directions of the gamma ray and the recoil nucleus relative to the incident beam. Subsequently Levinson and Bannerjee[9] have shown that the effect of distortions is to produce a correlation function $W(\theta) = A + B \sin^{2} 2(\theta_{\gamma} - \theta_{o})$. In this case the symmetry axis θ_{o} is not the direction of the recoil nucleus, but is usually close to it. Thus a measurement of the p'γ angular correlation in $0^{+} \longrightarrow 2^{+} \longrightarrow 0^{+}$ transitions should give a rather clear-cut indication of the existence of DI mechanisms in the inelastic scattering.

II. APPARATUS AND PROCEDURES

(i) Cyclotron and scattering chambers

The source of protons used in these experiments was the University of Rochester 27" variable energy cyclotron. The external beam may be focussed through a wedge analyzer into two scattering chambers placed in series along the beam pipe, or the unanalyzed beam may be focussed directly on to a target. The first scattering chamber, ten inches in diameter, may be used in conjunction with a broad range spectrometer magnet for high resolution work or the beam can be passed through this chamber into a 36 inch diameter chamber containing a scintillation counter on a rotating arm. For the $(p,p'\gamma)$ correlation measurements, a 6 inch diameter scattering chamber was situated before the analyzing magnet and the unanalyzed beam focussed on the target by a quadrupole lens. The energy calibration of the analyzed beam was accurate to about 0.5% and the energy spread was less than 0.5%. The energy spread of the unanalyzed beam in the 6 inch scattering chamber was approximately 100 kev. The alignment of the beam on the axis of counter rotation was checked at each chamber by observing the Coulomb scattering from a gold target. In each case, deviations from pure Coulomb scattering were less than the counting statistics of 3%.

(ii) Targets

The targets used and their properties of interest are listed in Table 1. Targets were all made relatively thick so that many levels would be excited in any CN process. For the targets with $A \geq 40$ it was estimated that at least 20 levels would be excited at the energies used in these measurements so that the statistical assumption should be a reasonable approximation. For Si^{28} and S^{32} only a few levels would likely be excited, and no attempt was made to interpret data from these targets with the statistical CN theory. Titanium targets of appropriate

thickness were commercially available. The isotopically enriched targets of nickel (Ni^{58} and Ni^{60}) were obtained from A.E.R.E., Aldermaston, England. The silicon target was made by blowing a thin bubble of Pyrex glass and selecting a fragment of appropriate thickness. This target contained appreciable amounts of impurities (mainly O^{16} and B^{11}) but at all angles of interest the proton group leading to the first excited state of Si^{28} was well resolved from all prominent contaminant groups. The sulfur target was made by evaporating sulfur onto a 0.01 mil gold leaf. To prevent the re-evaporation of sulfur during the proton bombardment, a thin layer of silver was evaporated over the sulfur. The Cu^{65} target was made by evaporating metallic Cu^{65}* onto a tungsten plate. After a sufficient thickness of Cu^{65} had accumulated on the plate, the copper film was easily peeled off to obtain a self-supporting foil. For the measurements on argon, commercially available argon gas (99. 99% pure) was used for the target material.

(iii) Angular distribution measurements

Most angular distributions were measured in the 36 inch chamber. The scintillation counter used in these measurements consisted of a 0.020 in. CsI(Tl) crystal bonded to the face of a DuMont-6291 photomultiplier. Pulses from this counter were amplified and analyzed in a RIDL model 3300 pulse height analyzer. Another scintillation counter mounted on a port at 45^{o} was used as a monitor.

For the A^{40} angular distribution measurements, the beam entering the scattering chamber passed through a collimating slit and two anti-scattering baffles. A thin nickel window covered the first baffle, and the second suppressed protons scattered by the nickel foil. The scattering chamber was filled with argon to a pressure of about 1/4 atmosphere.

---

* Obtained from Isotope Division, Oak Ridge National Laboratory, Oak Ridge, Tennessee.

The effective target volume was defined by a set of three collimating apertures mounted in front of the scintillation detector. It was not possible to make an experimental check of the alignment of these collimators, but over the angular range involved in these measurements, the error introduced by any misalignment was estimated to be less than 5%.

Typical spectra obtained with the scintillation counter are shown in figure 1. Prominent inelastic groups are seen, and the expected positions of protons elastically scattered from C and O have been labelled. Proton energies indicated are lab energies at the center of the target.

For the odd-even nucleus Cu^{65}, the broad range spectrometer magnet was used to resolve the rather closely spaced levels. This was also used for the angular distribution measurements at several forward angles for Ni^{58} and Ni^{60}. The spectrometer is a 90° broad range instrument of the Bainbridge-Buechner type, and uses nuclear emulsions to record the focussed particles. These measurements were carried out just after the installation of this magnet, before adequate anti-scattering baffles had been installed on the pole faces. As a result, at very forward angles the inelastic groups of interest were obscured by a serious background of particles scattered from the pole faces. Typical spectra obtained with the spectrometer magnet are shown in figure 2.

(iv) Angular correlation measurements

Angular correlations were measured in the 6 inch scattering chamber before the analyzer magnet. A slot 1/2 inch high covered by .001 inch Mylar foil extends from 20° to 160° on one side of this chamber to permit the observation of scattered protons. The other side of the chamber over this angular range was milled down to a thickness of 1/16" so that γ rays produced in the target could be detected outside the chamber with a minimum

of attenuation in the chamber wall. A port for a monitor counter was also provided which allowed the observation of particles scattered upwards at 45°.

The proton detector used was a thin (~1/16") NaI(Tl) crystal mounted on a DuMont-6291 photomultiplier. The gamma detector was a 2 inch by 1 1/2 inch diameter NaI(Tl) crystal mounted on a RCA-6810A photomultiplier. The centering of the gamma detector on the axis of the chamber, and the uniformity of the wall thickness was checked by measuring the angular distribution of gamma rays from a Co^{60} source mounted in the position of the target. This distribution was isotropic except for a decrease of 10% at the angle at which the target frame intercepted the gamma rays.

As is well known, the beam pulses from a cyclotron are generally sharply bunched. The duration of the individual pulses from this machine has been found to be one to two millimicroseconds at a cyclotron frequency of 20 mc. In order to monitor the accidental coincidence rate in this situation a special transistorized time-to-pulse height converter was used which allowed the observation of coincidences over the duration of several beam pulses before and after each inelastic proton count. A block diagram of the converter is shown in Fig. 3. The detailed description of the circuit will be published elsewhere.[10]

Pulses from the proton detector are clipped and amplified and go to univibrator A and single channel analyzer C which is set to accept pulses from the inelastic protons of interest. The output of univibrator A is a rectangular pulse of 650 μsec duration which unclamps univibrator B. Pulses from the gamma detector are clipped to a rise time of about 15 μsec, delayed in a variable delay line, and after amplification go to univibrator B. This univibrator is normally clamped off, but when unclamped by the output pulse a from univibrator A, produces a

rectangular output pulse b with width equal to the time difference between the start of the gamma pulse and the end of pulse a. Pulse b is fed to the first grid of a 6BN6, which is gated on by the output pulse from single channel analyzer C. The signal on the plate of the 6BN6 is integrated in a small capacitor to give an output pulse of amplitude proportional to the width of pulse b. After amplification this is fed to a multi-channel pulse height analyzer. In operation, the discrimination level at the input of univibrator A was set as low as possible to minimize time jitter in the appearance of pulse a. Univibrator B was set to respond to gamma ray pulses corresponding to an energy loss in the crystal of 0.4 Mev or more. The dead time of this converter was determined by the recovery of univibrators A and B and was equal to about 1.5 μsec. At the highest counting rates used in the measurements, counting losses in the circuit were less than 3%.

A schematic diagram of the output spectrum from this circuit is shown in Fig. 4, along with a typical spectrum from an actual measurement. The main advantage of this system for coincidence measurements with a pulsed beam is that the accidental rate can be determined for several successive beam pulses. The accidental rate was always found to be constant within statistics for successive pulses, and it was felt that this method provided a completely reliable measurement of the accidental rate.

III. RESULTS

(i) Angular Distributions

The measured angular distributions with error bars indicating the magnitude of the statistical uncertainties only are shown in Figs. 5 to 8. Large uncertainties were introduced at forward angles by the subtraction of the tail of the elastic peak, and this factor determined the smallest angle at which measurements could be made.

The following specific comments may be made regarding the individual measurements:

A^{40}: Angular distributions of protons leaving A^{40} in its first three excited states were measured at 6.14 Mev. The third excited state (Q = -2.66 Mev) has been tentatively identified previously[11] and its energy is confirmed in this measurement. Since this element has a rather low (p,n) threshold (2.29 Mev) it was expected that compound nucleus formation would result in the emission of neutrons rather than protons, so that inelastic scattering would proceed primarily by a DI. This expectation does not seem to be borne out by the measured angular distributions since in all cases these are almost symmetric about 90°. The absolute cross-sections for these levels were obtained by comparing the elastic and inelastic groups at forward angles, assuming the elastic scattering to pure Coulomb. The error introduced by this assumption may be as great as 30%, but would not likely be more than this. The important fact is that the absolute cross-sections are appreciably less than those for inelastic scattering to the first excited states of neighboring or heavier even-even nuclei (Ti^{48}, Cr^{52}, Ni^{58} or Ni^{60}) at these energies, but are still much greater than those to the excited states of Cu^{65}, at least at backward angles. This would suggest that neutron emission provides some competition to proton emission in the decay of the CN, but not as much as might be expected. It may be that the large spin

values of many of the low-lying states of K^{40} inhibit neutron emission.

Ni^{58} and Ni^{60}: Angular distributions of protons leading to the first excited state were measured at 4.70, 5.64 and ~6.7 Mev. In order to make measurements at forward angles at 6.8 Mev, the magnetic spectrometer was used. When the backward angle measurements were made with a scintillation detecotr, technical difficulties prevented cyclotron operation above 6.65 Mev, and it was necessary to combine these data at slightly different energies to obtain complete angular distributions. This procedure is at least reasonable, since the statistical assumption should be a good approximation at this energy, and that part of the scattering arising from CN formation should not change appreciably over such a small energy range. As a further check a measurement on Ni^{58} and Ni^{60} at 6.56 Mev with the scintillation counter showed distributions almost identical with those at 6.65 Mev. Absolute cross sections were again obtained by comparison of the inelastic groups with the elastic peak. The elastic cross sections at the energies of interest were obtained by interpolation from measurements for Ni^{58} at 7.8 Mev[12] and for natural nickel at 5.25[13] and 7.5[14] Mev. The uncertainty in these estimates is about 20%.

At 4.70 Mev, proton groups from carbon and oxygen contamination on the targets were resolved at all angles, and introduced no error into the measurements. At 5.64 and 6.7 Mev the group from carbon could not be resolved at backward angles, and since measurements of the cross section for elastic scattering of protons on C^{12} are not available over this energy range, it was not possible to make a subtraction for this contamination. Assuming that the cross section at backward angles is no more than a few times that at 90°, the maximum error in the measured cross sections would be no greater than 10%.

For both isotopes, the angular distributions at 4.69 and 5.64 Mev are very nearly symmetric about 90°, suggesting a predominant CN reaction mechanism. At ~6.7 Mev however, both show a slight but definite forward peaking. The peaking is more prominent for Ni^{60}, but it should be noted that the cross section at backward angles is considerably smaller for Ni^{60} than for Ni^{58}. The distributions for both isotopes may be interpreted as a DI contribution with a forward peak of about 5 mb/st superposed on an essentially isotropic CN background of about 5 mb/st for Ni^{60} and 10 mb/st for Ni^{58}. A possible reason for this difference in the CN cross sections is seen by comparing the scintillation spectra for Ni^{58} and Ni^{60} at 6.8 Mev. It is seen that scattering to excited states above the first is considerably more intense for Ni^{60}, so that protons from CN processes are spread over more exit channels in this case and the CN cross section to the first excited state is decreased.

Cu^{65}. DI contributions to the inelastic proton scattering on this target are expected to be more prominent relative to CN contributions than for the even-even nuclei studied since the low (p,n) threshold and many low-lying states in Cu^{65} provide many open channels for the decay of compound states. Since evidence of forward peaking was being sought, measurements were carried out at forward angles using the spectrometer magnet, and no effort was made to extend the measurements beyond the angle at which the elastic group from carbon contamination became troublesome. For the first excited state group, the background of protons scattered inside the spectrometer was also severe, and no measurements were made on this group. Measurements were possible from 45° to 90° for the group to the second excited state and to 120° for that to the third.

The absolute cross section for each group was estimated to be 0.55 ± .2 mb/st at 90°. This is smaller by a factor of ten than the

usual cross sections for even-even nuclei in this region, and indicates the effect of the many open (p,n) and (pp') channels in decreasing the CN cross section to any one final state. Both of these angular distributions show a marked forward peaking, indicating a predominant DI reaction mechanism.

(ii) Angular Correlations

The results of the correlation measurements for Si^{28}, S^{32}, Ti^{48}, Ni^{58} and Ni^{60} are shown in Figs. 9 to 17. The errors in these measurements arise almost completely from counting statistics, and these are shown as the error bars in the figures. Except for the data on Ni^{58} at 5.7 Mev, the solid curves represent least-square fits of the experimental data to a correlation function of the DI form $W(\theta) = A + B \sin^2 2(\theta - \theta_o)$. In each case fits were carried out for several values of θ_o in order to obtain a best fit with respect to all three parameters A, B and θ_o. A slight correction for finite geometry[15] was then applied to each fitted curve to yield the formula written on each figure for the true correlation function. Results of the fitting are summarized in Table 2. To check the validity of fitting these data to the assumed correlation function, a χ^2 test was performed for each measurement. Correlations for which χ^2 was less than the value corresponding to a 1% probability of no better fit are indicated as "yes" in the "χ^2 test" column Table 2. Errors quoted for A and B are rms deviations. Values of $\Delta\theta_o$ listed in the table were determined by the requirement that the probability of no better fit for $\chi^2(\theta_o \pm \Delta\theta_o)$ should be half that for $\chi^2(\theta_o)$.

A statistical CN correlation function was used to fit the measurements on Ni^{58} at 5.7 Mev. Explicit formulas for such correlations are given by Seward[1]. In order to simplify the calculations it was assumed that only two decay channels (inelastic scattering to the first excited state, and compound elastic scattering) were open, and furthermore only partial waves with

$L, L' \leq 2$ were taken into account. Optical model transmission coefficients[16] were used, yielding the correlations shown in Fig. 14. The most prominent features of these correlations are the approximate symmetry about 90°, with a rather pronounced dip near 90°. In the present case, these result from the relatively large contribution (~50%) to the $0^+ \longrightarrow 2^+$ transition arising from an incident D wave and outgoing S wave. It is worth noting explicitly that correlations in CN processes in general do not show symmetry about 90° either for a single level in the CN or for a superposition of many levels.

Again some of the important points of the individual measurements may be noted:

Si^{28} All angular correlations at center of mass energies of 5.66 and 6.7 Mev could be fitted with a correlation function of the DI form. The differences between θ_0 and the classical angle of the recoil nucleus, θ_R, are less than 12° except for the data at $E_{pcm} = 5.66$ Mev, $\theta_{p'} = 135^\circ$ where the correlation is so slight that the symmetry axis is not well defined. The measured θ_0 approximately follow θ_R as the angle of the inelastically scattered proton is varied and do not change as the energy is varied.

These results differ somewhat from those of Bowsher et al[4] apparently because of differences in energy and target thickness. They are however consistent with their conclusion that a DI is important in this reaction at these energies.

S^{32} The measured correlations at $\theta_{p'} = 90^\circ$ and 135° are both fitted very well with a DI form but with a symmetry axis quite different from θ_R. These results are similar to those of Hausman et al[3] at 6.5 Mev. Equally good fits to the data are obtained however if it is assumed that the scattering proceeds through a single resonance of spin $3/2^+$ or $5/2^+$ with an incident D wave and outgoing S wave. On the basis of these

few results, it is not possible to conclude how important a DI may be in this reaction.

Ti^{48} Since the excitation energy of the CN V^{49} is about 13 Mev in these measurements the statistical assumption is probably reasonable for this case. The measured correlation functions for $\theta_{p'} = 90^{\circ}$ at both 5.72 and 6.77 Mev are almost symmetric about 90° with minima near 90°. These are far from the simple DI prediction which gives a maximum at about 90°, and suggest that a CN mechanism is predominant at $\theta_{p'} = 90^{\circ}$. The correlation function at $\theta_{p'} = 135^{\circ}$ and at 5.72 Mev shows the DI form but with a symmetry axis midway between the predictions of the simple DI and the statistical CN theory. At 6.77 Mev, the measured correlation can not be fitted with the form $A + B \sin^2 2(\theta - \theta_o)$ and is not symmetric about any axis.

Ni^{58} The correlations at 5.73 Mev do not show the DI form, but have a shallow minimum at 90° for all $\theta_{p'}$. All are fitted well with the predictions of the statistical CN theory, and support the earlier conclusion that at this energy inelastic scattering proceeds mainly via CN processes. At 6.8 Mev, the correlation for $\theta_{p'} = 45^{\circ}$ and 135° appears to show the DI form, but with the symmetry axis shifted about 20° from the classical recoil angle. Actually the value of χ^2 obtained in fitting the data at $\theta_{p'} = 45^{\circ}$ is large enough to indicate that the DI form of the correlation is not completely satisfactory.

Ni^{60} The correlations in this case are generally similar to those for Ni^{58}. The correlations at 5.73 Mev were fitted by a DI form, but it is seen that they would be consistent with the statistical CN prediction also. At 6.8 Mev, the correlation for $\theta_{p'} = 90^{\circ}$ is almost isotropic. For this case the DI correlation should show a maximum at $\theta_{\gamma} = 90^{\circ}$ and the CN correlation a minimum. It may be that the observed result represents a mixing of comparable DI and CN contributions. The data at the

other proton angles is also consistent with this interpretation though these correlations are close to the DI form since the minima in the DI and CN correlations are separated by smaller angles than for $\theta_{p'} = 90^{o}$.

DISCUSSION

These results, along with earlier work in this energy range by Seward[1], and by Hausman et al[2-4] indicate that the DI mechanism may be quite important in inelastic proton scattering at relatively low energies. On the basis of his correlation measurements on Mg^{24} and Cr^{52} Seward has suggested that the relative importance of CN and DI processes is determined by the ratio of the energies of incident and emergent particles to the Coulomb barrier height. The present results on Si^{28} and Ni^{58} and Ni^{60} also indicate the DI processes become important once the energy of the incident proton is about equal to the barrier height. It is interesting to observe the energy dependence of the angular distributions for Ni^{58} and Ni^{60} over a wider energy range by combining the present data with other data between 8 and 15 Mev[12,17] as shown in Figs. 18 and 19. All angular distributions above 8 Mev show definite forward peakings with the ratio of forward to backward yield decreasing gradually as the energy is decreased. At 6.8 Mev there are still weak but appreciable forward peakings and the distributions become essentially isotropic at 5.64 and 4.70 Mev. A qualitative explanation of this result may be given by considering the form of the expression for the cross section for the two types of reaction mechanisms.

For a CN mechanism, the results of Hauser and Feshbach[18] give a cross section proportional to a sum of terms of the form $TT'/\sum \epsilon T''$ where T and T' are barrier penetrabilities for the incident and outgoing protons and ϵ is a channel spin factor. The sum in the denominator is taken over all open channels for the decay of the CN.

For a DI, the cross section is proportional to the absolute square of a transition matrix element $T_{fi} \propto \int \psi_f^* \phi_f^* V \phi_i \psi_i \, dr \, dr'$ where ψ_i and ψ_f are wave functions of the target and residual nuclei, ϕ_i and ϕ_f are wave functions of incident and scattered nucleons respectively, and V is the interaction potential. Hence the cross section will be proportional to the product of the squares of the wavefunctions for incident and emergent particles, evaluated at the position of the nucleus, which is essentially just the product of the barrier penetrabilities TT' for incident and outgoing particles. Thus the ratio σ_{DI}/σ_{CN} becomes proportional to $TT'/TT'/\sum \epsilon T'' = \sum \epsilon T''$ This factor is close to zero when the incident proton energy is below the coulomb barrier height and increases rapidly as the energy increases above the coulomb barrier height. For the Ni isotopes, the coulomb barrier height is about 6.5 Mev and the experimental data show a marked increase of σ_{DI}/σ_{CN} above this energy.

Although these results on the Ni isotopes indicate the importance of the Coulomb barrier in determining the ratio σ_{DI}/σ_{CN} a comparison of data from different nuclei at the same energy shows the importance of other factors. Specifically, angular distribution and correlation for Cr^{52} at 7.02 Mev obtained by Seward[1] show less evidence for a DI than do the data for the Ni isotopes at 6.8 Mev in spite of the lower coulomb barrier of Cr. This effect is also seen in the inelastic scattering measurement by Hu et al[19] and Kobayashi et al[17] between 8 and 14 Mev. Angular distributions for Ti, Cr, Fe, Ni, and Zn all show a definite forward peaking, but at all energies the peaking of the Ni and Zn distributions is much more pronounced than in those for Ti and Cr.

For a direct collective excitation in inelastic scattering, Pinkston and Satchler[20] have pointed out that the expression for the transition amplitude is similar in form to that for the electromagnetic

transition amplitude between the same states. Fig. 20 shows a plot of the differential cross sections at the forward peak for the 14 Mev data versus the reduced E2 transition probabilities[21] for these elements. No measurement of the E2 probability for Cr^{52} was available, though the small values reported for Cr^{53}[21] and Cr^{54}[22] indicate that it will also be small. The correlation between these quantities suggests that a DI involving a collective excitation is the predominant mechanism in these reactions at 14 Mev. The appearance of the angular distributions and correlations at 7 Mev then indicates that this DI may still be important at 7 Mev in spite of large CN contributions at this energy. Below 6 Mev however, DI contributions apparently are negligible.

Angular distributions of protons scattered inelastically from Mg^{24} and Si^{28} have also been measured at energies up to 14 Mev[23]. For these light elements prominent resonances are observed and the energy variation of the angular distributions does not show the simple regular behaviour observed for elements around A = 60. Nevertheless, the cross sections show a forward peaking at 14 Mev, and the peak cross section for Mg^{24} is somewhat greater than that for Si^{28}. It has also been found that Mg^{24} and Si^{28} show E2 transition rates much greater than the single particle values, with Mg^{24} showing the greater enhancement[24-26]. Thus the strong angular correlations observed for both Mg and Si even in the energy region in which prominent CN resonances occur may reasonably be interpreted as evidence of a strong collective DI in the inelastic scattering from these nuclei.

TABLE I. Properties of Targets Used in the Measurements

target	thickness (mg/cm^2)	isotopic abundance (%)	excited state studied	energy of ex. state (Mev)	spin gnd state	spin ex state	excitation in CN for 0 energy proton (Mev)	(p,n) threshold (Mev)
Si^{28}	.5	92.28	1st	1.78	0+	2+	2.724	15.4
S^{32}	1	95.06	1st	2.24	0+	2+	2.285	14.2
A^{40}	0.5 1.0	99.6	1st	1.46	0+	(2+?)	7.800	2.29
			2nd	2.22		(2+)		
			3rd					
Ti^{48}	2.2	73.4	1st	0.99	0+	2+	6.73	4.80
Ni^{58}	1.8	95	1st	1.45	0+	(2+)	3.42	9.459
Ni^{60}	2.2	95	1st	1.332	0+	2+	4.79	7.028
Cu^{65}	15	98.2	2nd	1.114	3/2-	(7/2-)	8.908	2.170
			3rd	1.482		(5/2, 7/2-)		

Target	$E_{p_{C.M.}}$ (Mev)	$\theta_{p'}$	A	B	B/A	$\theta_o \pm \Delta\theta_o$	$\theta_o - \theta_R$	X^2 Test
Si^{28}	5.66	45°	305 ± 6	115 ± 10	0.38 ± 0.04	66° ± 6°	12°	Yes
		90°	206 ± 4	179 ± 12	0.87 ± 0.06	41° ± 3°	2°	Yes
		135°	132 ± 5	33 ± 10	0.25 ± 0.08	INDEFINITE		Yes
	6.7	45°	201 ± 11	310 ± 19	1.54 ± 0.12	67° ± 1°	12°	Yes
		90°	136 ± 7	245 ± 13	1.80 ± 0.14	41° ± 1°	1°	Yes
		135°	280 ± 11	131 ± 17	0.47 ± 0.065	14° ± 3°	-6°	Yes
S^{32}	5.66	90°	185 ± 11	196 ± 16	1.06 ± 0.10	0° ± 2°	-36°	Yes
		135°	204 ± 12	224 ± 17	1.10 ± 0.12	2° ± 2°	-16.5°	Yes
Ti^{48}	5.72	90°	268 ± 7	23 ± 10	0.086 ± 0.036	88° ± LARGE	50.5° ± LARGE	Yes
		135°	219 ± 7	127 ± 10	0.58 ± 0.05	9° ± 5°	-11°	Yes
	6.77	90°	186 ± 7	110 ± 10	0.59 ± 0.06	80° ± 4°	42°	Yes
Ni^{58}	6.8	45°	136 ± 15	233 ± 22	1.72 ± 0.25	78° ± 2°	19°	No
		135°	169 ± 7	188 ± 8	1.11 ± 0.06	0° ± 3.5°	-21°	Yes
Ni^{60}	5.73	90°	254 ± 6	90 ± 7	0.35 ± 0.032	1° ± 7°	-40°	Yes
		135°	205 ± 10	107 ± 14	0.52 ± 0.075	5° ± 3°	-15.5°	Yes
	6.8	50°	224 ± 20	203 ± 31	0.91 ± 0.14	71° ± 3°	13°	No
		135°	162 ± 13	152 ± 19	0.94 ± 0.16	11° ± 2°	-10°	Yes

Table 2. Results of fitting correlation measurements to the DI form.

References

1. F. D. Seward, Phys. Rev. 114, 514 (1959).

2. H. A. Lackner, G. F. Dell, and H. J. Hausman, Phys. Rev. 114, 560 (1959).

3. H. J. Hausman, G. F. Dell, and H. F. Bowsher, Phys. Rev. 118, 1237 (1960).

4. H. F. Bowsher, G. F. Dell, and H. J. Hausman, Phys. Rev. 121, 1504 (1961).

5. See for example, H. Feshbach, Nuclear Spectroscopy Part B (Edited by Fay Ajzenberg-Selove) Academic Press, Page 661.

6. S. Devons and L. J. B. Goldfarb, Handbuch der Physik XLII, Springer, Berlin, 362 (1957).

7. N. Austern, S. Butler, and H. McManus, Phys. Rev. 92, 350 (1953).

8. G. R. Satchler, Proc. Phys. Soc. London, A68, 1037 (1955).

9. C. A. Levinson and M. K. Banerjee, Annals of Physics, 2, 499 (1957); 3, 67 (1958).

10. Hiroshi Taketani, "A Coincidence Analyser for use with Pulsed Accelerators", NYO-9750 (1961), to be published.

11. I. J. Van Heerden and D. J. Prowse, Phil. Mag. 1, 967 (L) (1956).

12. G. W. Greenless and P. M. Rolph, Proc. Phys. Soc. 75, 201 (1960).

13. D. A. Bromley and N. S. Wall, Phys. Rev. 102, 1560 (1956).

14. W. F. Waldorf and N. S. Wall, Phys. Rev. 107, 1602 (1957).

15. M. E. Rose, Phys. Rev. 91, 610 (1953).

16. C. A. Preskitt and W. P. Alford, Phys. Rev. 115, 389 (1959).

17. S. Kobayashi et al, Journ. Phys. Soc. Japan, 15, 1151 (1960).

18. W. Hauser and H. Feshbach, Phys. Rev. 87, 366 (1952).

19. C. H. Hu et al., Journ. Phys. Soc. Japan 14, 861 (1959).

20. W. T. Pinkston and G. R. Satchler; Proceedings of the International Conference on Nuclear Structure, Kingston, Canada, (1960), p. 394. The relationship between inelastic scattering cross section and E2 transition rates was first pointed out by B. L. Cohen and A. G. Rubin, Phys. Rev. 111, 1568 (1958).

21. C. A. Mallmann, Nucl. Phys. 24, 535 (1961).

22. D. S. Andreyev et al., Nucl. Phys. 19, 400 (1960).

23. Y. Oda et al., Journ. Phys. Soc. Japan 15, 760 (1960).

24. S. Devons, G. Manning, and J. H. Towle, Proc. Phys. Soc. (London) A69, 173 (1956).

25. R. H. Helm, Phys. Rev. 104, 1466 (1956).

26. G. Rakavy, Nucl. Phys. 4, 375 (1957).

FIGURE CAPTIONS

Fig. 1. - Proton spectra measured with scintillation counter.

Fig. 2. - Proton spectra measured with broad range spectrograph.

Fig. 3. - Block diagram of time to pulse height converter used in p'γ coincidence measurements.

Fig. 4. - The upper curve illustrates the expected spectrum from the circuit of Figure 3. The lower curve shows the result of a measurement.

Fig. 5. - Angular distributions of protons inelastically scattered to the first three excited states of A^{40} at 6.14 Mev.

Fig. 6. - Angular distributions or protons inelastically scattered to the second and third excited states of Cu^{65} at 6.83 Mev.

Fig. 7. - Angular distributions of protons inelastically scattered to the first excited state of Ni^{58} at energies of 4.70, 5.64 and ~6.7 Mev. The curves simply connect the measured points.

Fig. 8. - Angular distributions of protons inelastically scattered to the first excited state of Ni^{60} at energies of 4.69, 5.63 and ~6.7 Mev. The curves are drawn to connect the measured points.

Fig. 9. - Angular correlations between inelastic protons and decay gamma rays for Si^{28} at 5.66 Mev.

Fig. 10 - Angular correlations between inelastic protons and decay gamma rays for Si^{28} at 6.70 Mev.

Fig. 11 - Angular correlations between inelastic protons and decay gamma rays for S^{32} at 5.66 Mev.

Fig. 12 - Angular correlations between inelastic protons and decay gamma rays for Ti^{48} at 5.72 Mev.

Fig. 13 - Angular correlations between inelastic protons and decay gamma rays for Ti^{48} at 6.77 Mev.

Fig. 14 - Angular correlations between inelastic protons and decay gamma rays for Ni^{58} at 5.73 Mev. The curves show the correlations predicted by the statistical CN theory.

Fig. 15 - Angular correlations between inelastic protons and decay gamma rays for Ni^{58} at 6.8 Mev.

Fig. 16 - Angular correlations between inelastic protons and decay gamma rays for Ni^{60} at 5.73 Mev.

Fig. 17 - Angular correlations between inelastic protons and decay gamma rays for Ni^{60} at 6.8 Mev.

Fig. 18 - Energy dependence of inelastic proton scattering on Ni^{58}. The forward peak shows a cross section of between 5 and 10 mb/steradian at all energies above 6 Mev.

Fig. 19 - Energy dependence of inelastic proton scattering on Ni^{60}.

Fig. 20 - Correlation between measured peak cross section for inelastic scattering and the corresponding reduced E2 transition rate.

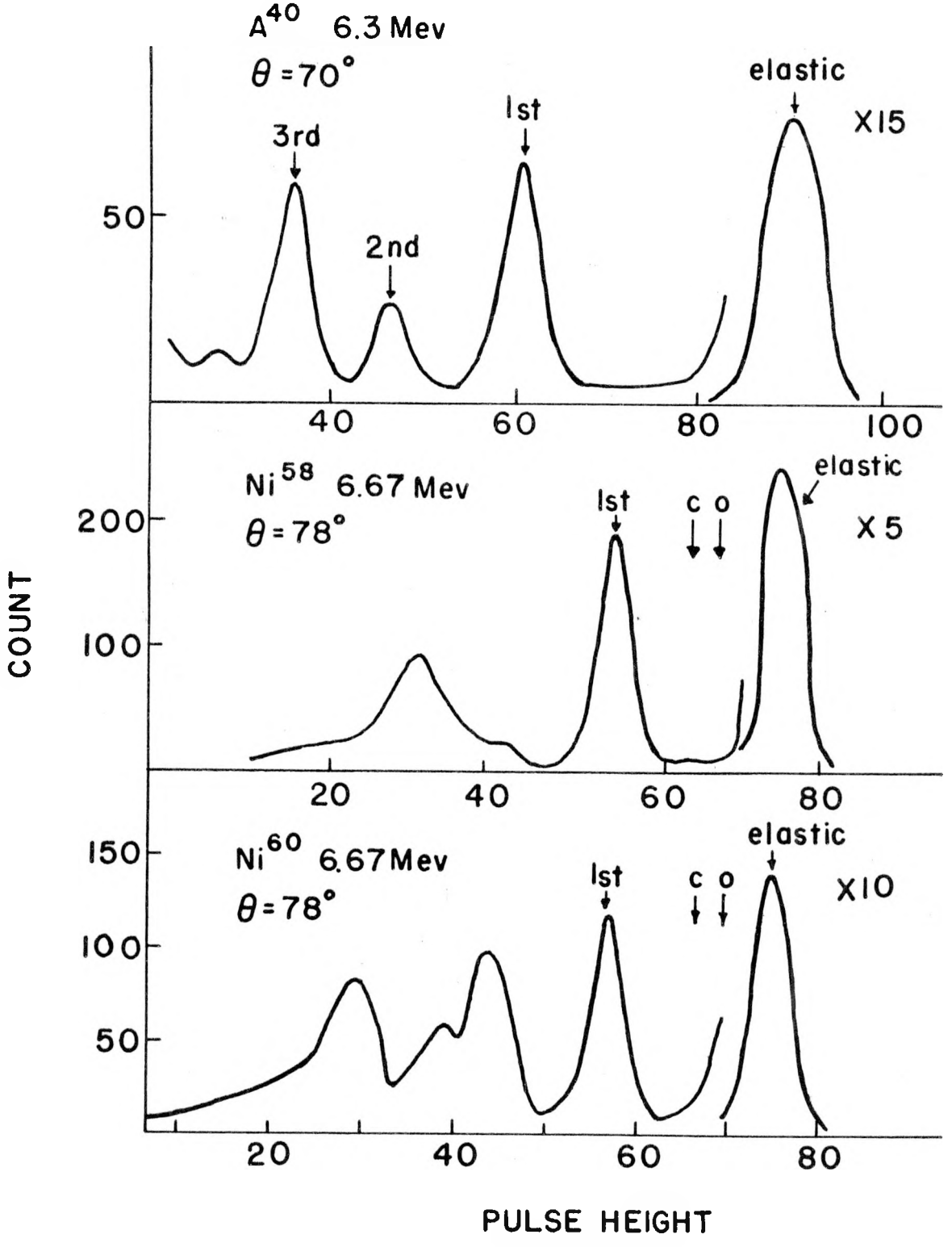
A40 6.3 Mev
θ = 70°
3rd
2nd
1st
elastic
X15
50
40
60
80
100
Ni58 6.67 Mev
θ = 78°
1st
C
O
elastic
X5
200
100
20
40
60
80
Ni60 6.67 Mev
θ = 78°
1st
C
O
elastic
X10
150
100
50
20
40
60
80
COUNT
PULSE HEIGHT

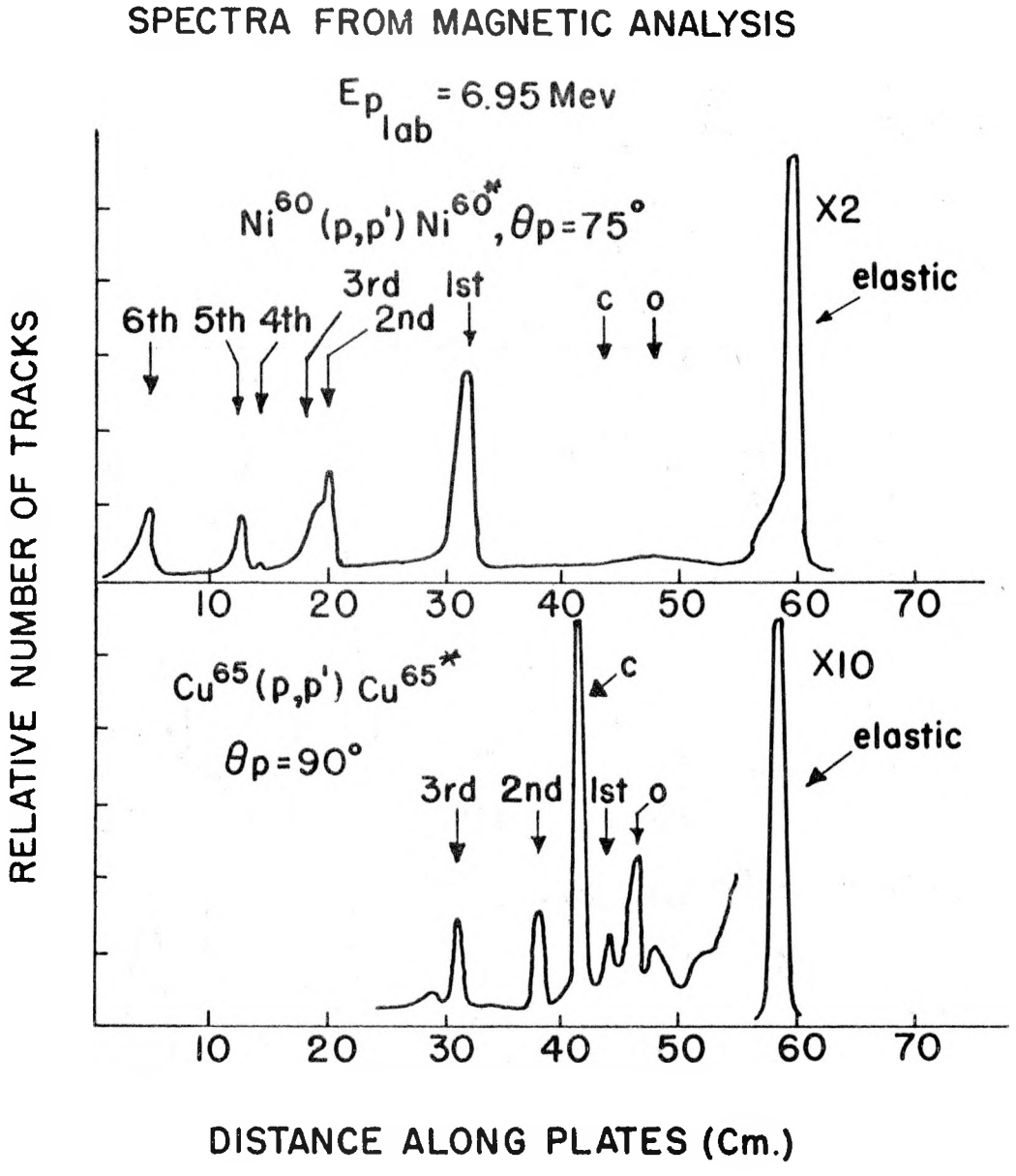
SPECTRA FROM MAGNETIC ANALYSIS
$E_{p_{lab}}$ = 6.95 Mev
$Ni^{60}(p,p')Ni^{60*}$, θ_p=75°
6th
5th
4th
3rd
2nd
1st
c
o
X2
elastic
10
20
30
40
50
60
70
$Cu^{65}(p,p')Cu^{65*}$
θ_p=90°
3rd
2nd
1st
c
o
X10
elastic
RELATIVE NUMBER OF TRACKS
DISTANCE ALONG PLATES (Cm.)

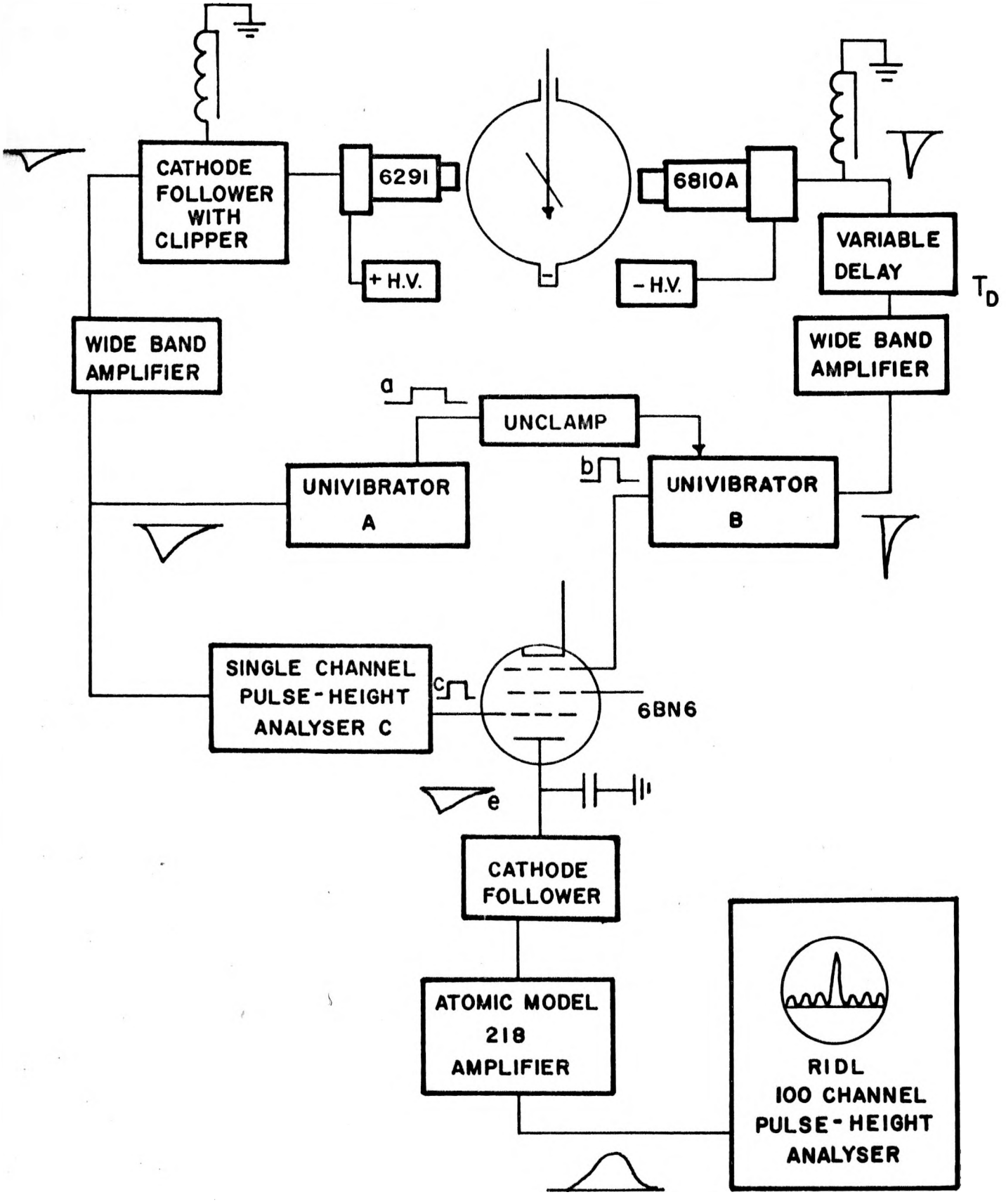
CATHODE FOLLOWER WITH CLIPPER
6291
6810A
+ H.V.
- H.V.
VARIABLE DELAY
T_D
WIDE BAND AMPLIFIER
WIDE BAND AMPLIFIER
a
UNCLAMP
b
UNIVIBRATOR A
UNIVIBRATOR B
SINGLE CHANNEL PULSE-HEIGHT ANALYSER C
c
6BN6
e
CATHODE FOLLOWER
ATOMIC MODEL 218 AMPLIFIER
RIDL 100 CHANNEL PULSE-HEIGHT ANALYSER

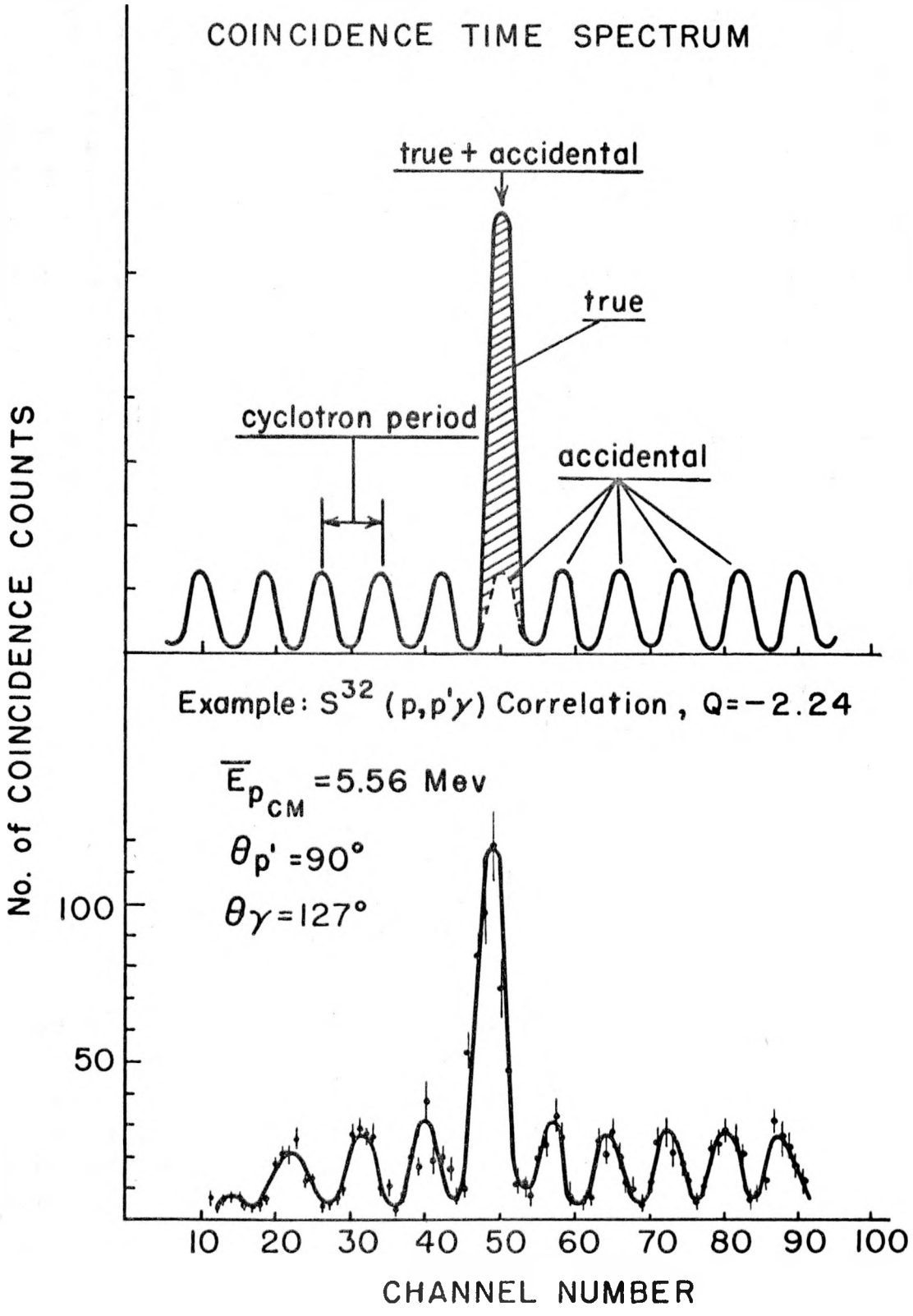
COINCIDENCE TIME SPECTRUM
true + accidental
true
cyclotron period
accidental
Example: S32 (p,p'γ) Correlation , Q=−2.24
$\overline{E}_{p_{CM}}$ =5.56 Mev
$\theta_{p'}$ =90°
θ_{γ} =127°
No. of COINCIDENCE COUNTS
100
50
10 20 30 40 50 60 70 80 90 100
CHANNEL NUMBER

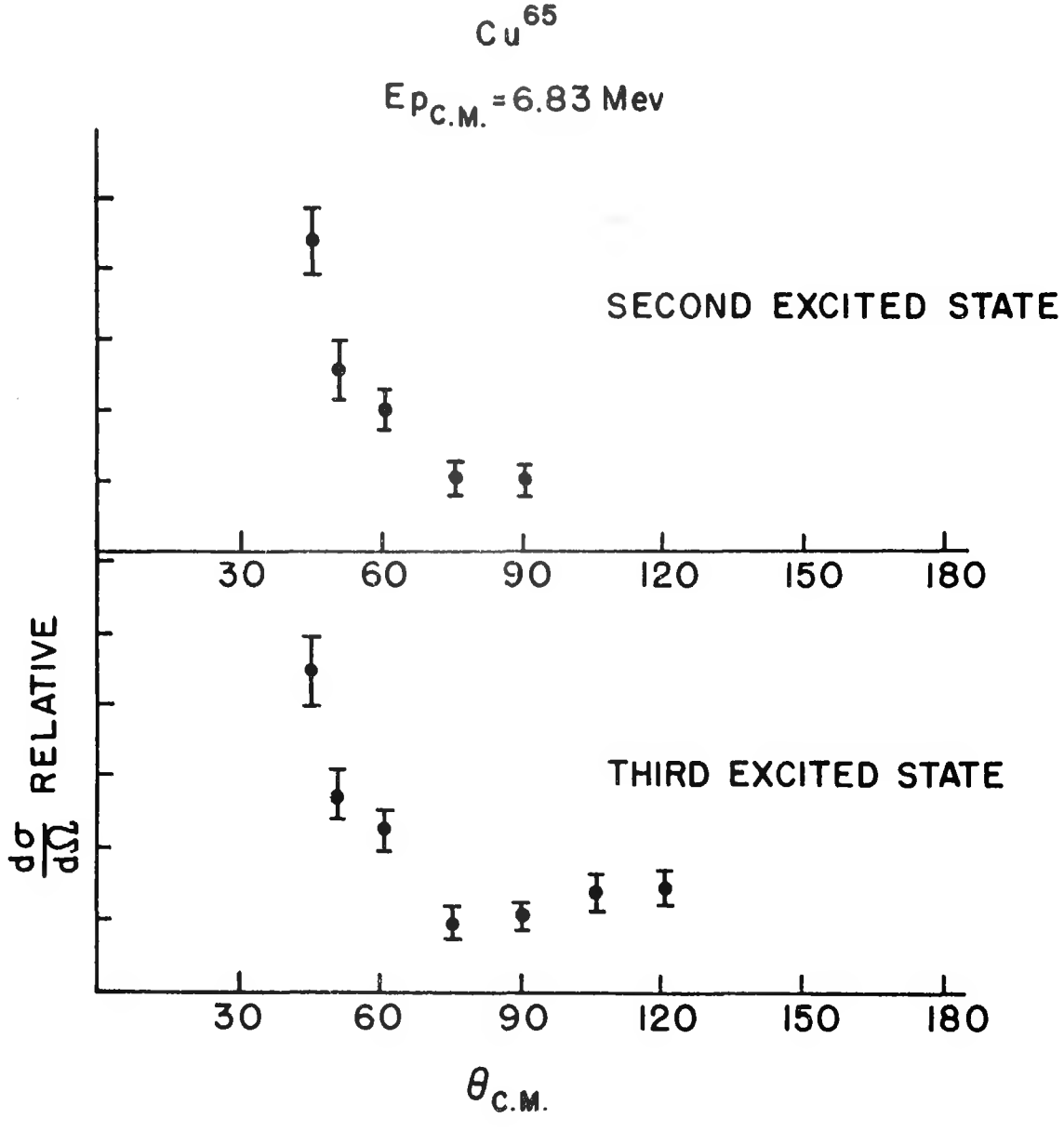
Cu^{65}
$Ep_{C.M.}$ = 6.83 Mev
SECOND EXCITED STATE
THIRD EXCITED STATE
30
60
90
120
150
180
$\frac{d\sigma}{d\Omega}$ RELATIVE
$\theta_{C.M.}$

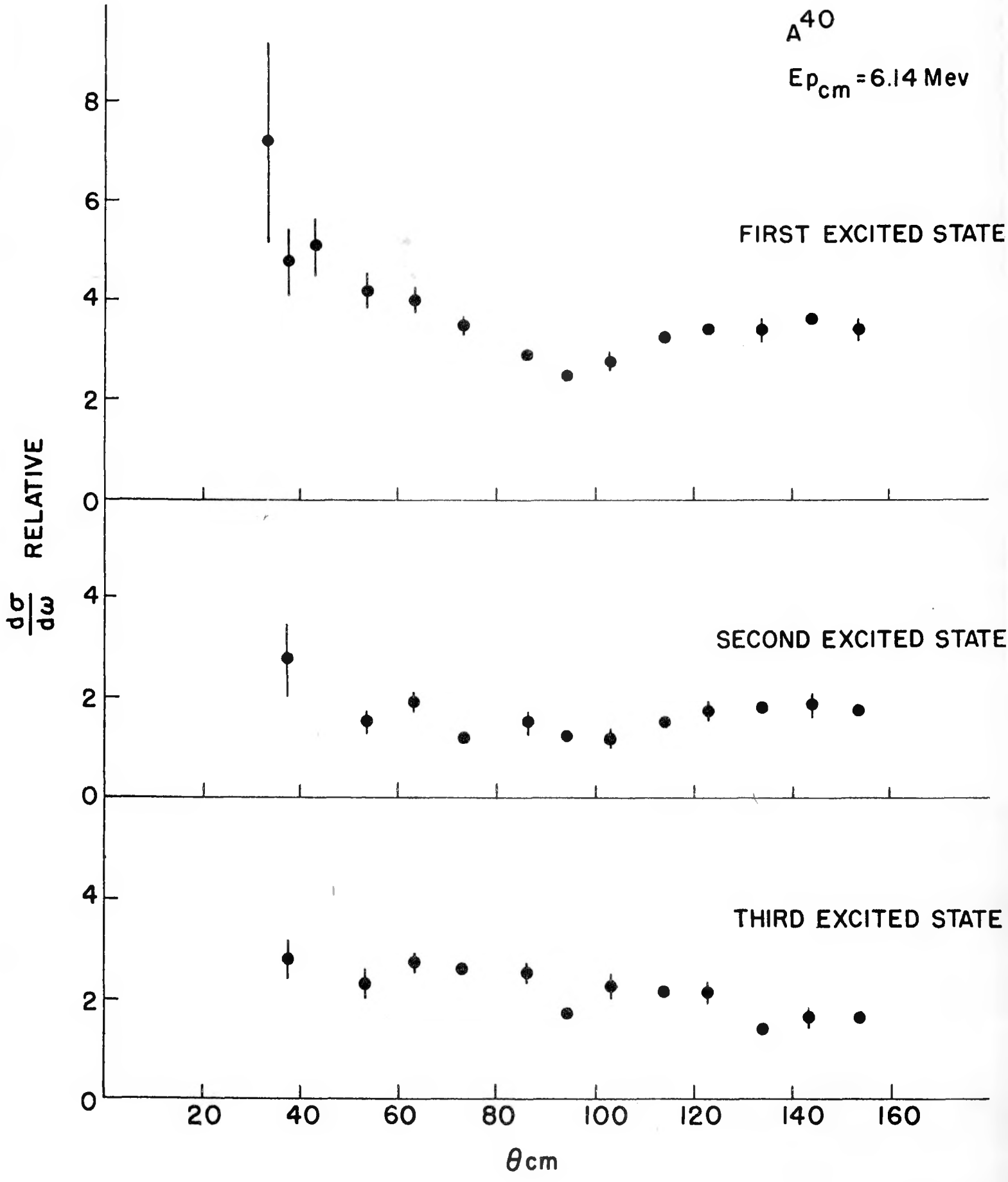
A^{40}
Ep_{cm} = 6.14 Mev
FIRST EXCITED STATE
SECOND EXCITED STATE
THIRD EXCITED STATE
$\frac{d\sigma}{d\omega}$ RELATIVE
0
2
4
6
8
20
40
60
80
100
120
140
160
θcm

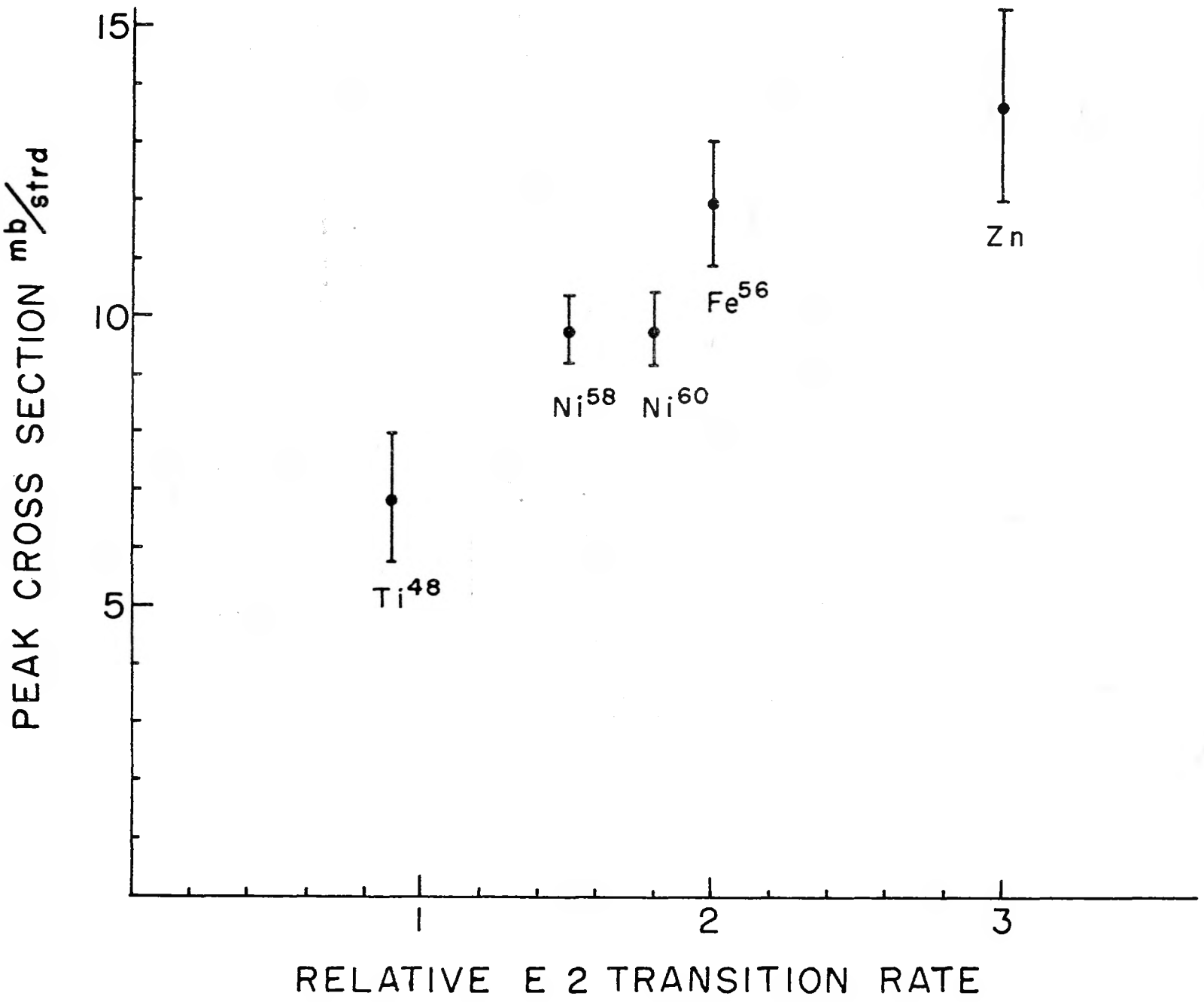
15
10
5
PEAK CROSS SECTION mb/strd
Ti48
Ni58
Ni60
Fe56
Zn
1
2
3
RELATIVE E 2 TRANSITION RATE

ENERGY DEPENDENCE OF ANGULAR DISTRIBUTIONS IN $Ni^{60}(p,p')Ni^{60*}_{1st}$

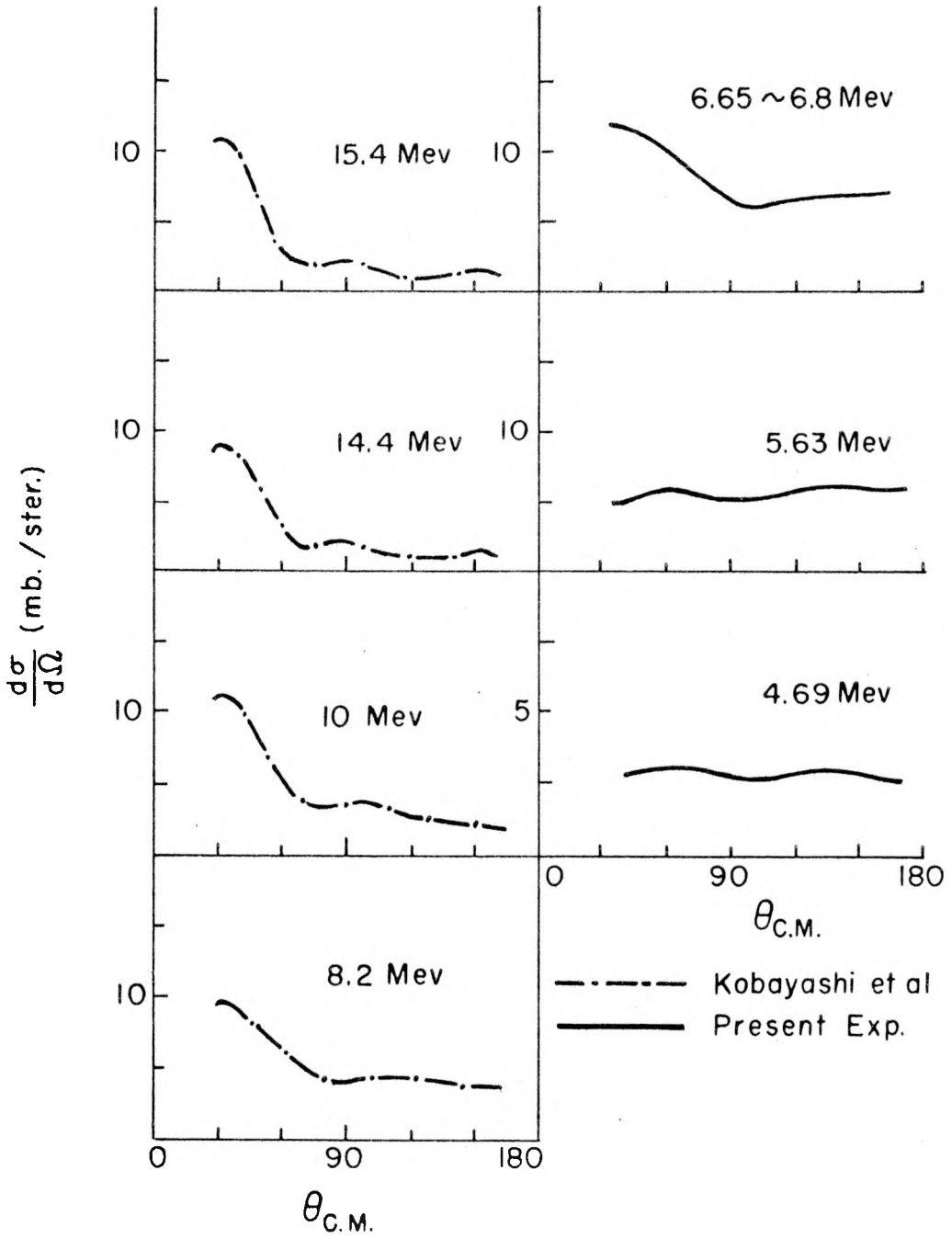

ENERGY DEPENDENCE OF ANGULAR DISTRIBUTIONS IN $Ni^{58}(p,p')Ni^{58*}_{1st}$

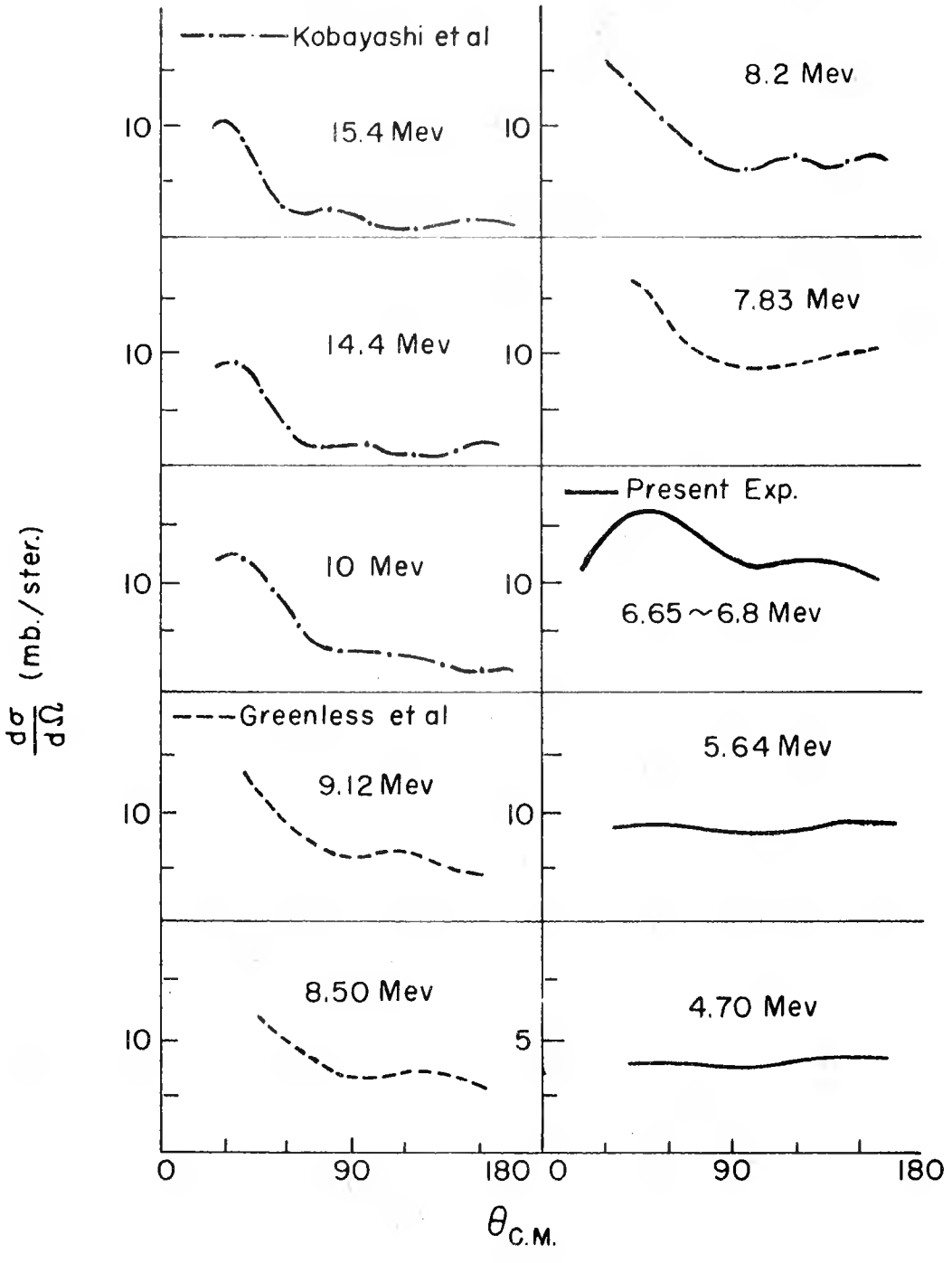

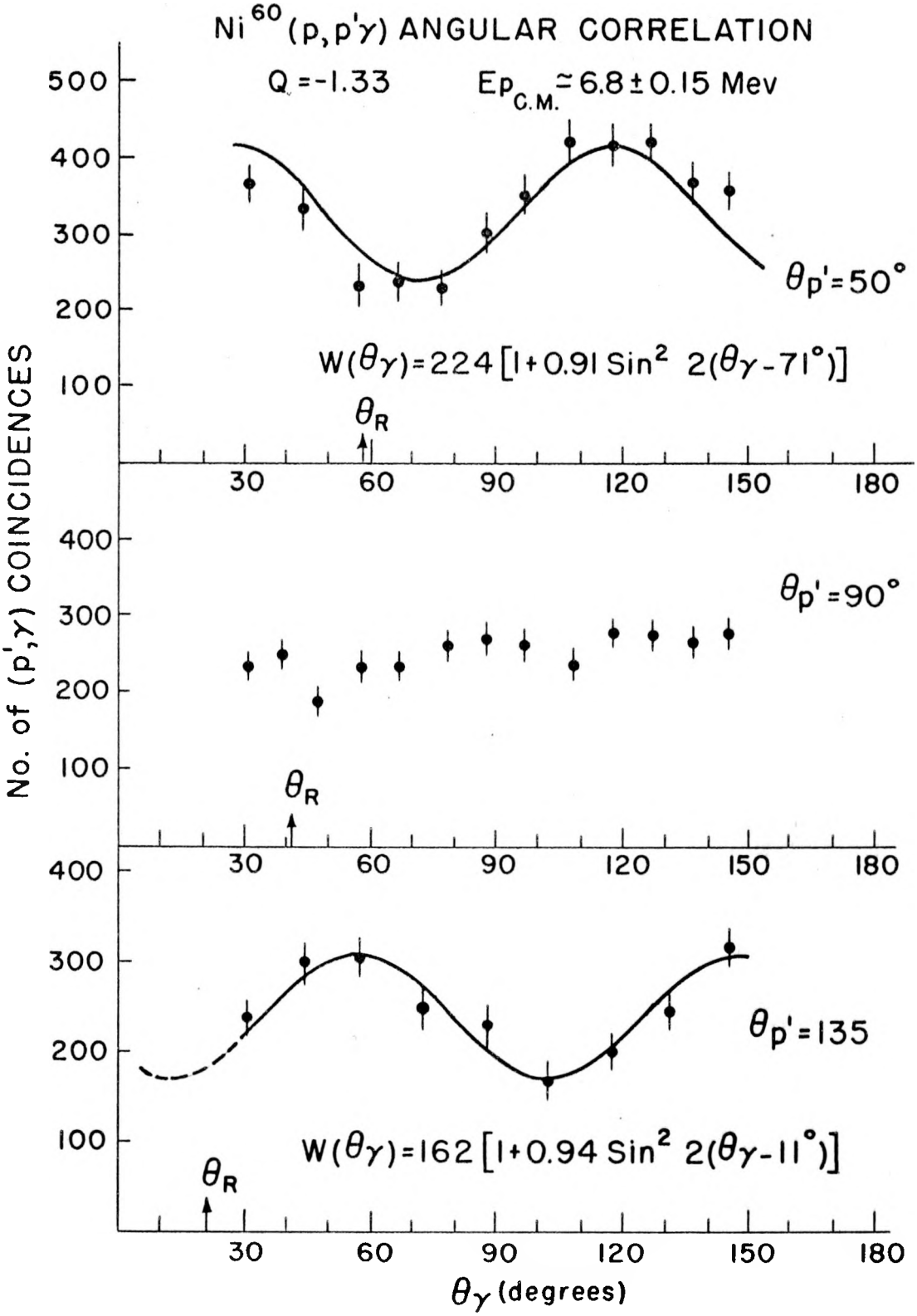
Ni 60 (p, p'γ) ANGULAR CORRELATION
Q = -1.33
Ep C.M. ≃ 6.8 ± 0.15 Mev
θp'=50°
W(θγ)=224 [1+0.91 Sin² 2(θγ-71°)]
θR
θp'=90°
θR
θp'=135
W(θγ)=162 [1+0.94 Sin² 2(θγ-11°)]
θR
No. of (p',γ) COINCIDENCES
θγ (degrees)
500
400
300
200
100
30
60
90
120
150
180

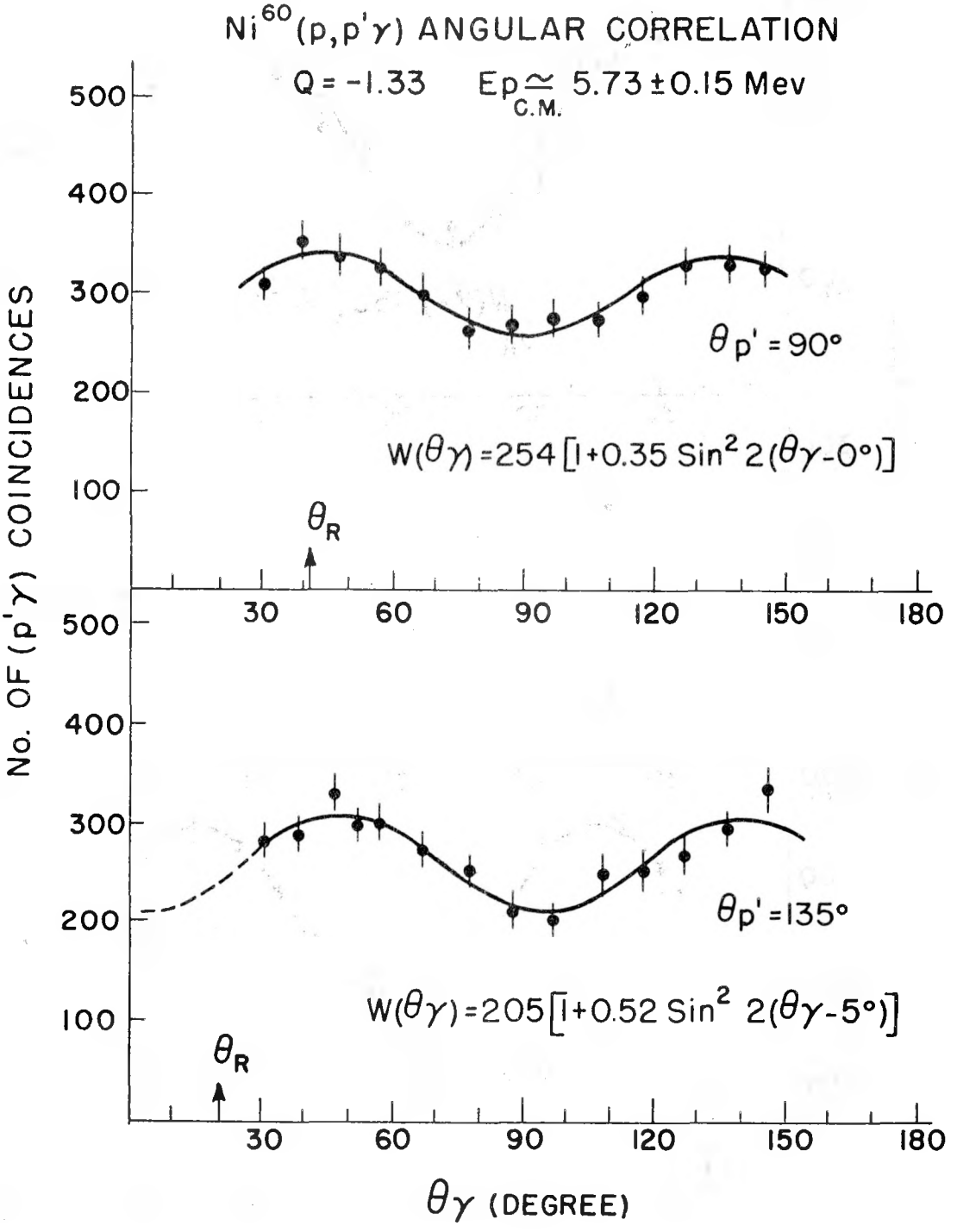
Ni^{60}(p,p'γ) ANGULAR CORRELATION
Q = -1.33 Ep$_{C.M.}$ ≃ 5.73 ± 0.15 Mev
No. OF (p'γ) COINCIDENCES
θp' = 90°
W(θγ) = 254 [1 + 0.35 Sin^2 2(θγ - 0°)]
θR
θp' = 135°
W(θγ) = 205 [1 + 0.52 Sin^2 2(θγ - 5°)]
θR
θγ (DEGREE)

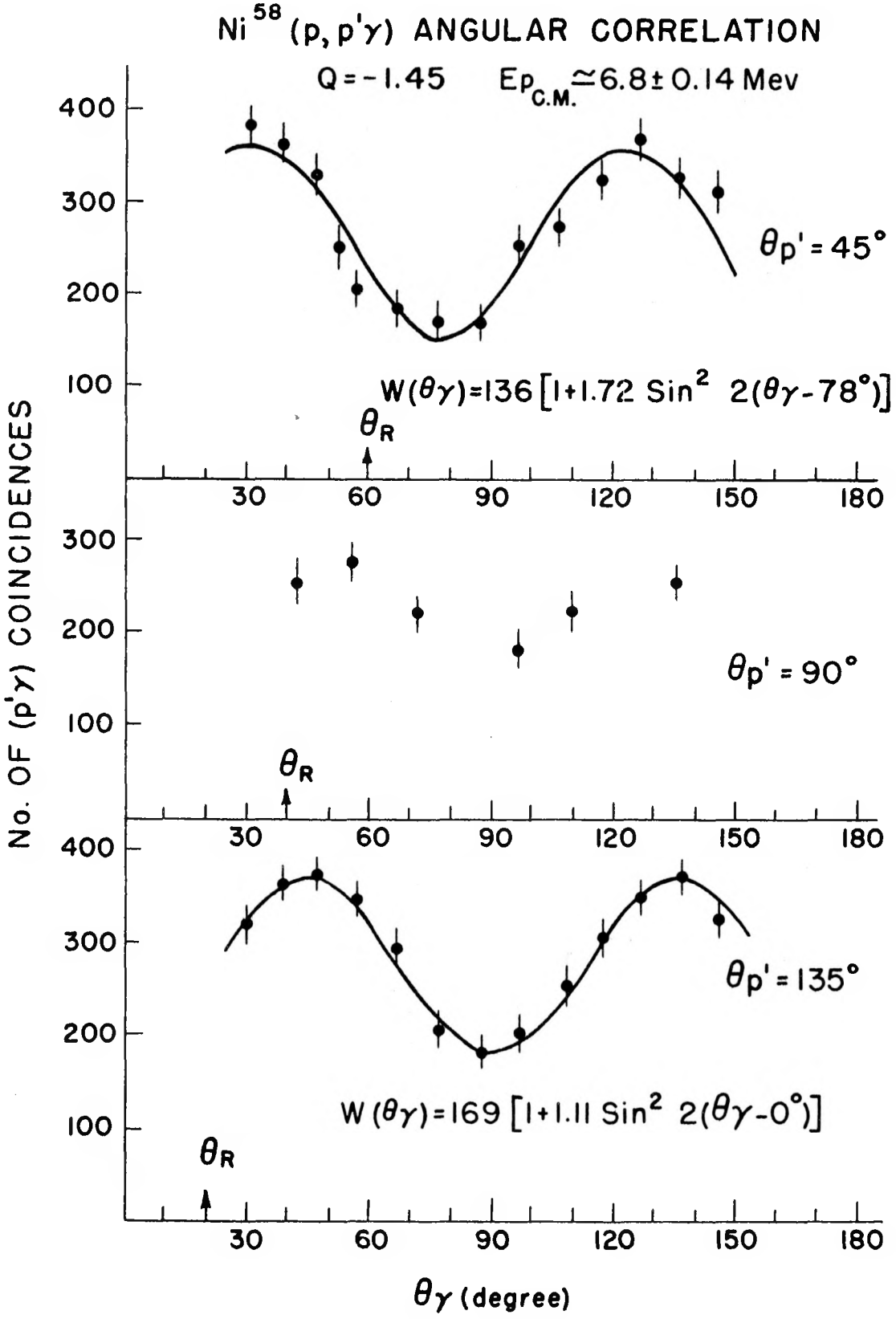
Ni 58 (p, p'γ) ANGULAR CORRELATION
Q = -1.45 Ep C.M. ≃6.8 ± 0.14 Mev
θp' = 45°
W(θγ)=136 [1+1.72 Sin² 2(θγ-78°)]
θp' = 90°
θp' = 135°
W (θγ)=169 [1+1.11 Sin² 2(θγ-0°)]
θR
No. OF (p'γ) COINCIDENCES
θγ (degree)
100
200
300
400
30
60
90
120
150
180

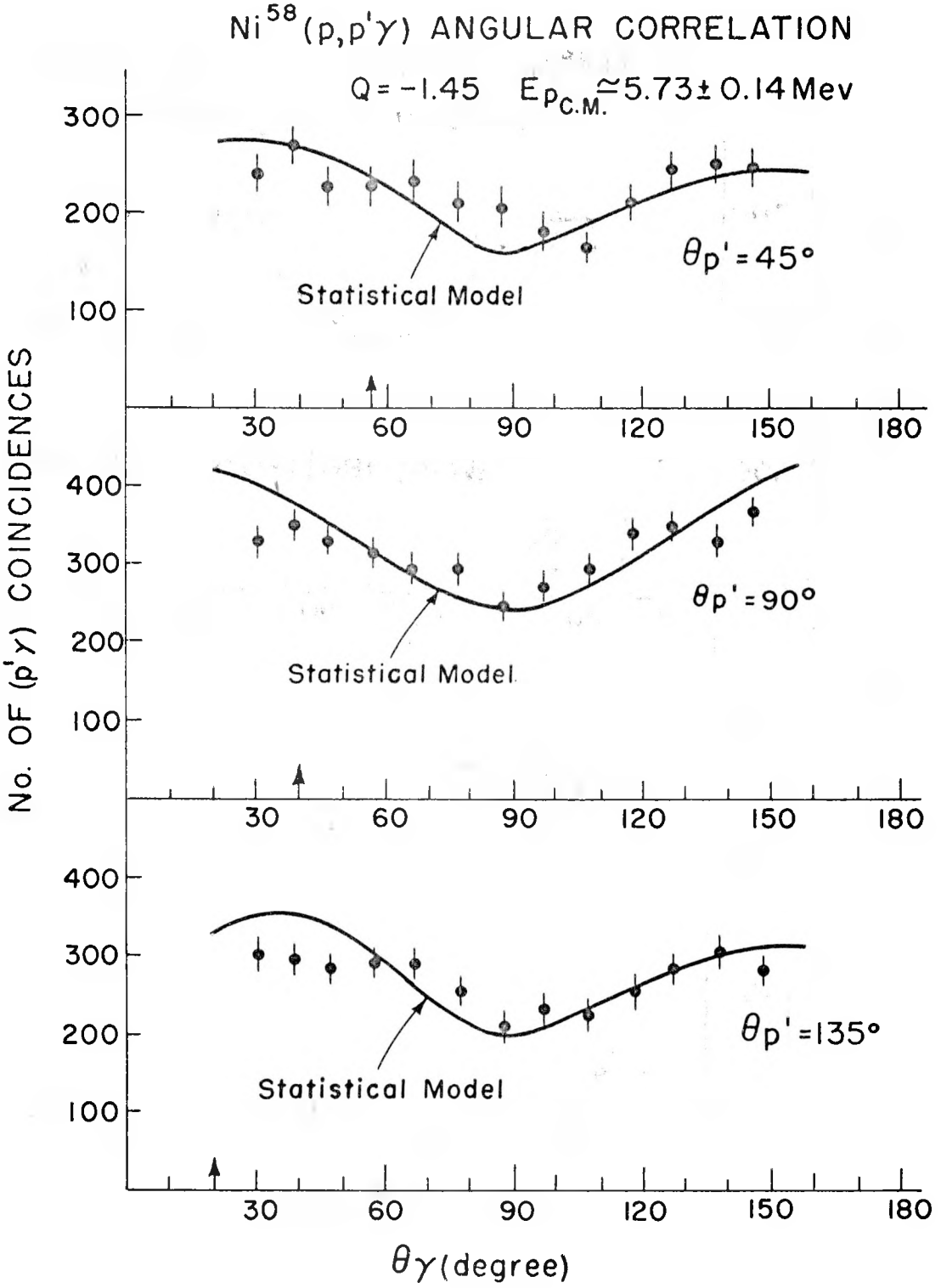
Ni^{58}(p,p'γ) ANGULAR CORRELATION
Q = −1.45 $E_{p_{C.M.}} \simeq 5.73 \pm 0.14$ Mev
No. OF (p'γ) COINCIDENCES
300
200
100
Statistical Model
$\theta_{p'} = 45°$
30
60
90
120
150
180
400
300
200
100
Statistical Model
$\theta_{p'} = 90°$
400
300
200
100
Statistical Model
$\theta_{p'} = 135°$
$\theta\gamma$ (degree)

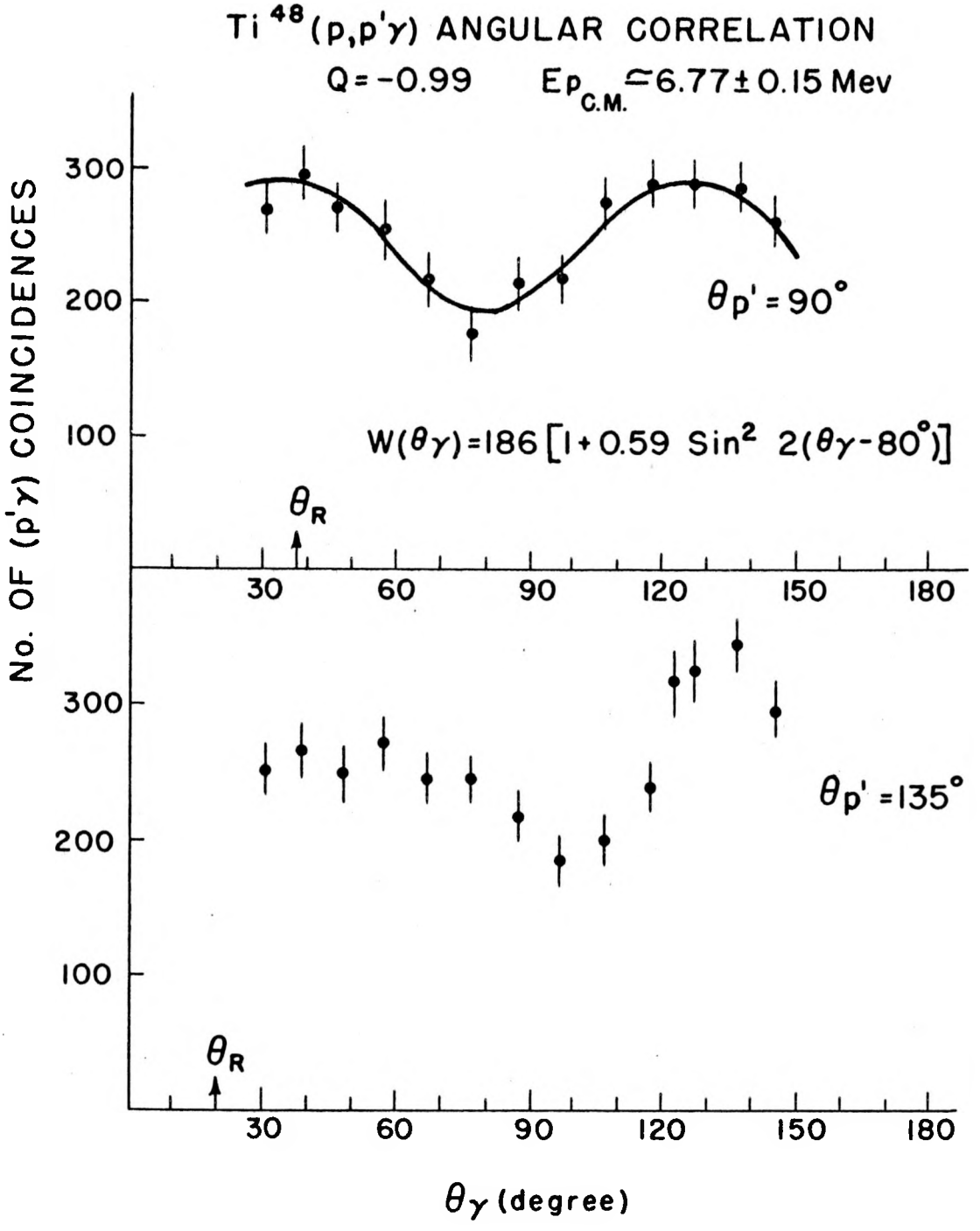
Ti 48 (p,p'γ) ANGULAR CORRELATION
Q = -0.99
Ep C.M. ≃ 6.77 ± 0.15 Mev
No. OF (p'γ) COINCIDENCES
300
200
100
θp' = 90°
W(θγ) = 186 [1 + 0.59 Sin² 2(θγ - 80°)]
θR
30
60
90
120
150
180
300
200
100
θp' = 135°
θR
30
60
90
120
150
180
θγ (degree)

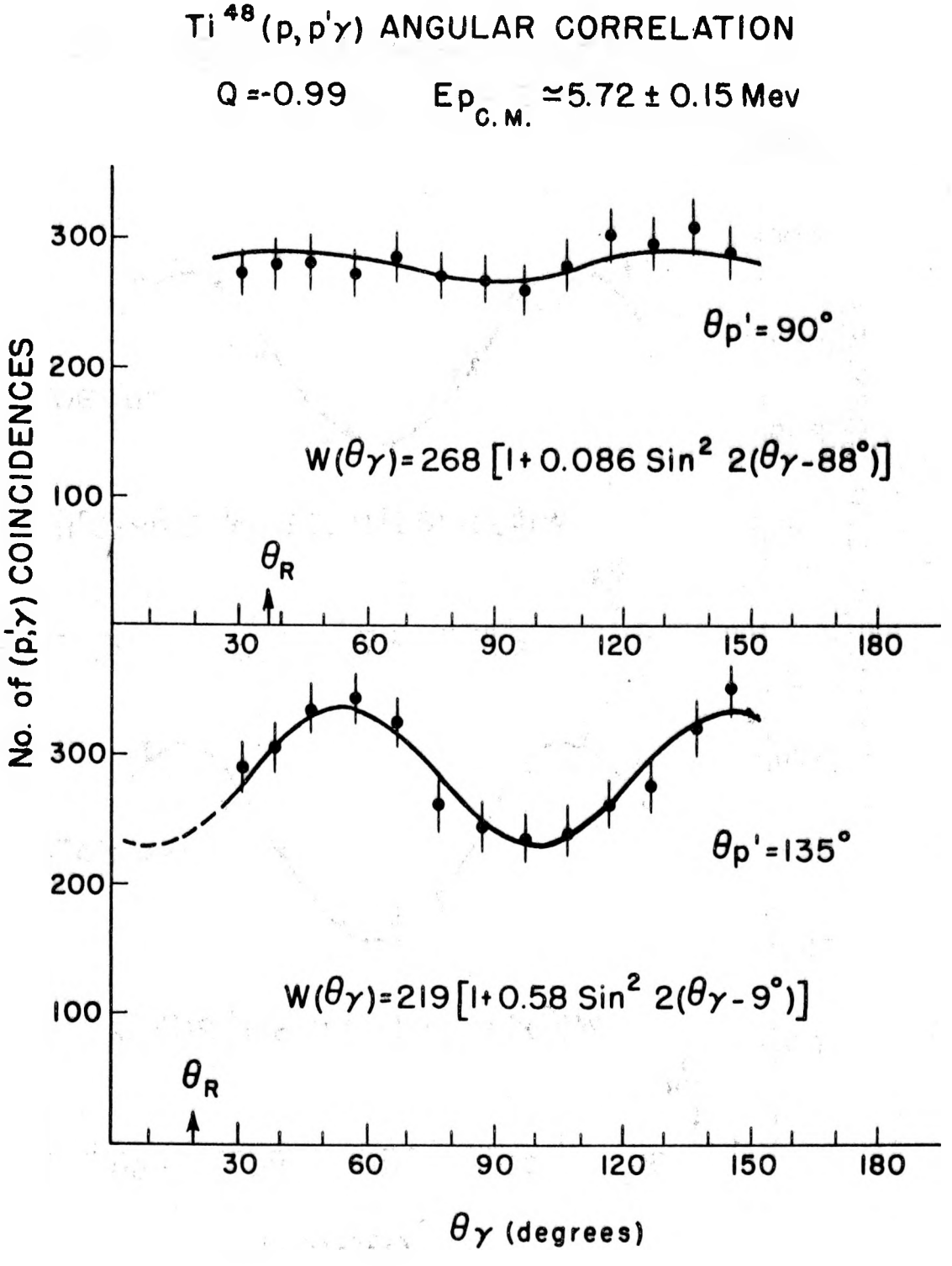
Ti 48 (p, p'γ) ANGULAR CORRELATION
Q =-0.99
Ep C. M. ≃5.72 ± 0.15 Mev
No. of (p,γ) COINCIDENCES
300
200
100
θp' = 90°
W(θγ) = 268 [1 + 0.086 Sin² 2(θγ - 88°)]
θR
30
60
90
120
150
180
300
200
100
θp' = 135°
W(θγ) = 219 [1 + 0.58 Sin² 2(θγ - 9°)]
θR
30
60
90
120
150
180
θγ (degrees)

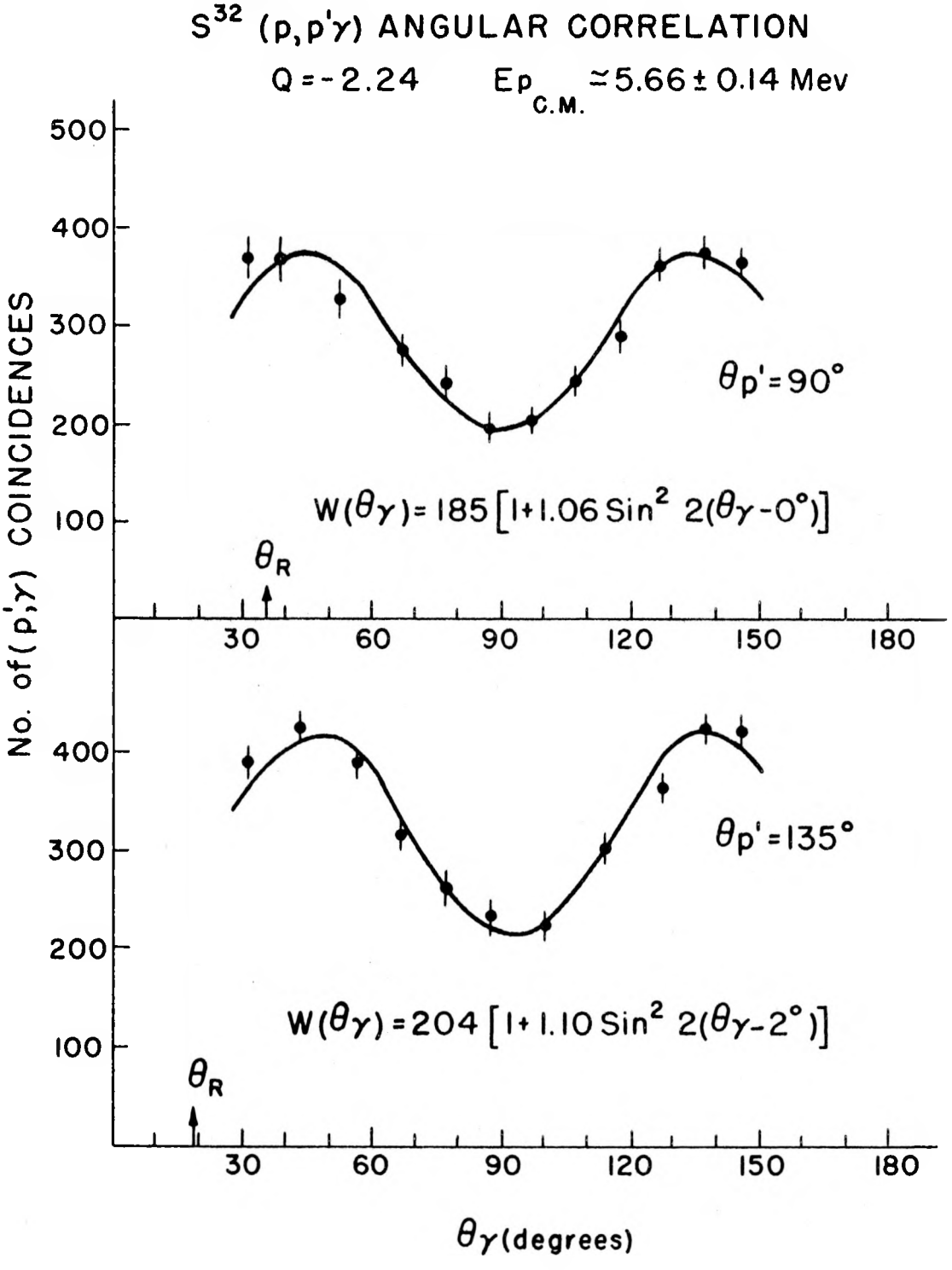
S^{32} (p,p'γ) ANGULAR CORRELATION
Q = -2.24
$Ep_{C.M.} \simeq 5.66 \pm 0.14$ Mev
No. of (p',γ) COINCIDENCES
500
400
300
200
100
$\theta_{p'} = 90°$
$W(\theta_\gamma) = 185\,[1 + 1.06 \sin^2 2(\theta_\gamma - 0°)]$
θ_R
30
60
90
120
150
180
400
300
200
100
$\theta_{p'} = 135°$
$W(\theta_\gamma) = 204\,[1 + 1.10 \sin^2 2(\theta_\gamma - 2°)]$
θ_R
30
60
90
120
150
180
θ_γ (degrees)

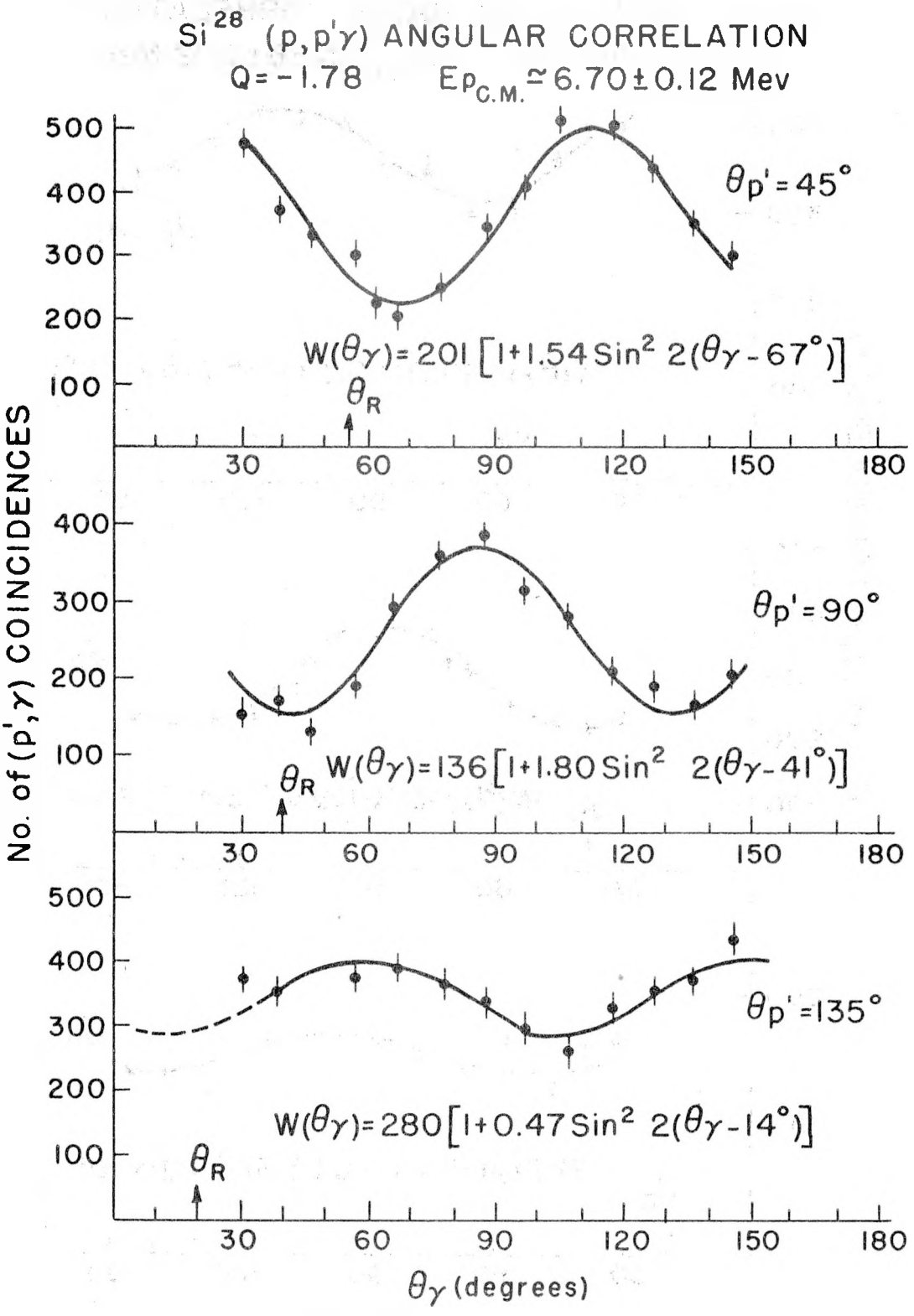
Si 28 (p,p'γ) ANGULAR CORRELATION
Q = -1.78 Ep C.M. ≃ 6.70 ± 0.12 Mev
θp' = 45°
W(θγ) = 201 [1 + 1.54 Sin² 2(θγ - 67°)]
θR
θp' = 90°
W(θγ) = 136 [1 + 1.80 Sin² 2(θγ - 41°)]
θR
θp' = 135°
W(θγ) = 280 [1 + 0.47 Sin² 2(θγ - 14°)]
θR
No. of (p',γ) COINCIDENCES
θγ (degrees)
100
200
300
400
500
30
60
90
120
150
180

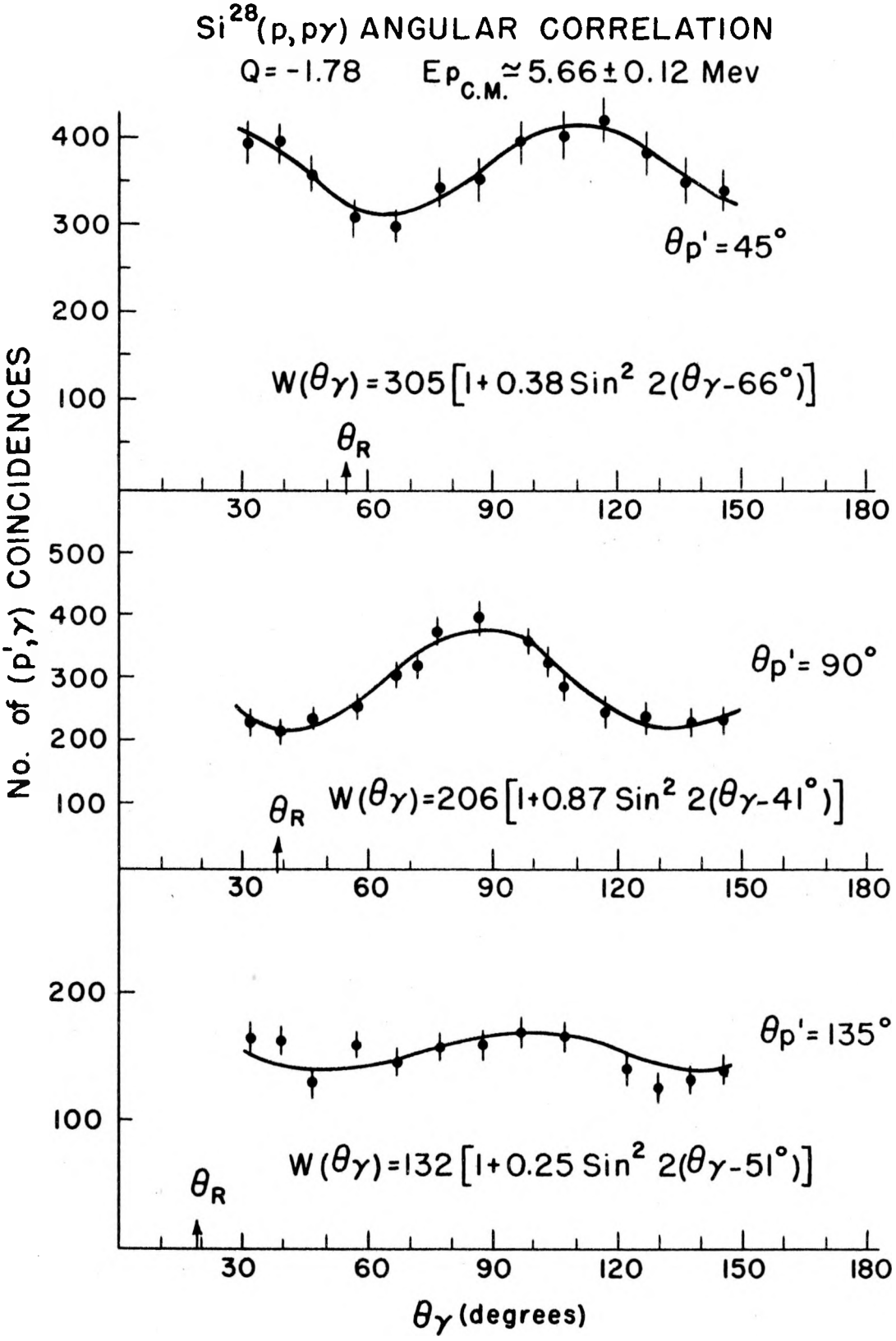
Si^{28}(p, pγ) ANGULAR CORRELATION
Q = -1.78 Ep$_{C.M.}$ ≃ 5.66 ± 0.12 Mev
No. of (p', γ) COINCIDENCES
400
300
200
100
θp' = 45°
W(θγ) = 305 [1 + 0.38 Sin² 2(θγ - 66°)]
θR
30
60
90
120
150
180
500
400
300
200
100
θp' = 90°
θR
W(θγ) = 206 [1 + 0.87 Sin² 2(θγ - 41°)]
30
60
90
120
150
180
200
100
θp' = 135°
W(θγ) = 132 [1 + 0.25 Sin² 2(θγ - 51°)]
θR
30
60
90
120
150
180
θγ (degrees)

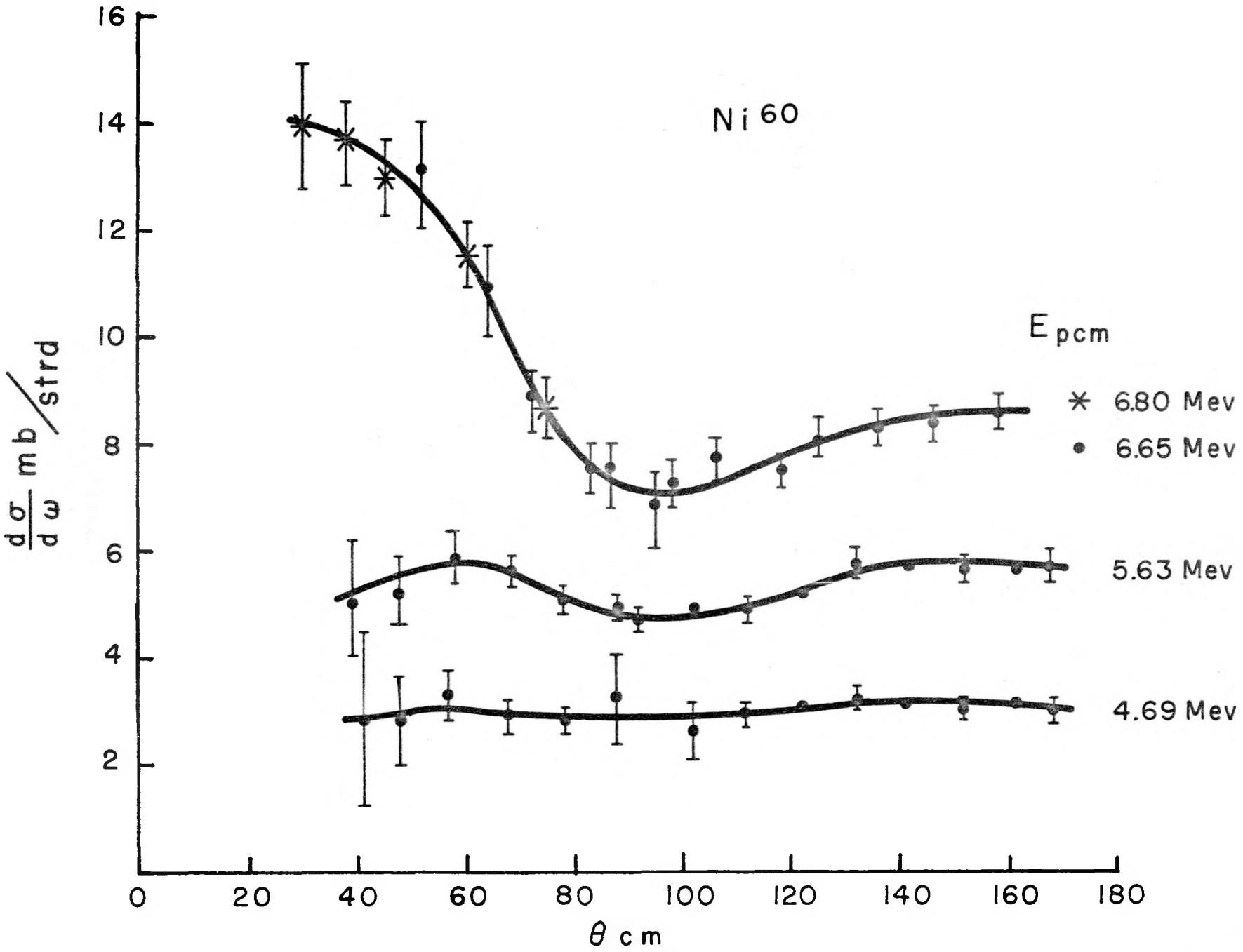
Ni 60
E pcm
6.80 Mev
6.65 Mev
5.63 Mev
4.69 Mev
dσ/dω mb/strd
θ cm
0
20
40
60
80
100
120
140
160
180
2
4
6
8
10
12
14
16

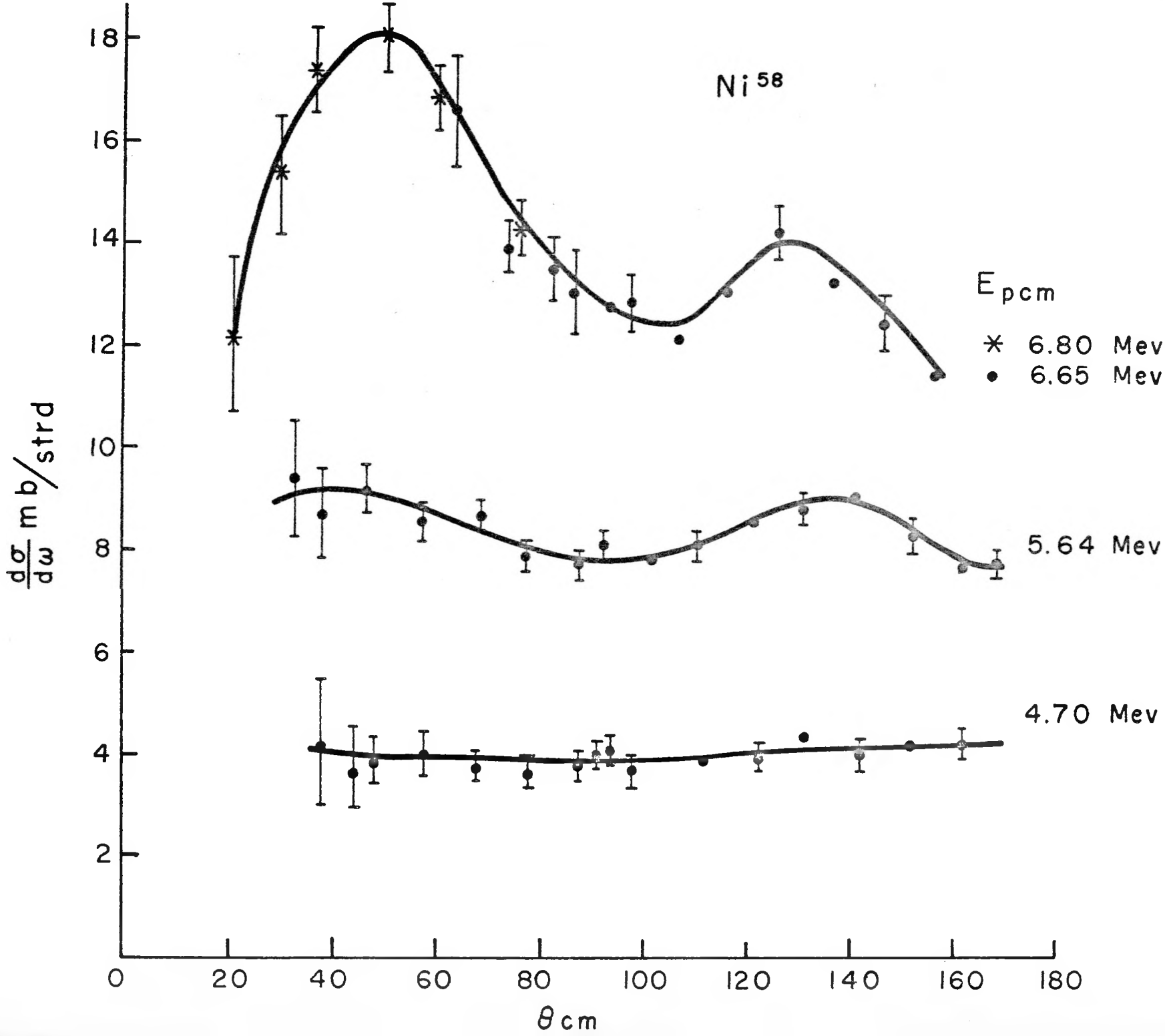
Ni 58
E_{pcm}
* 6.80 Mev
• 6.65 Mev
5.64 Mev
4.70 Mev
$\frac{d\sigma}{d\omega}$ mb/strd
θ cm
0
20
40
60
80
100
120
140
160
180
2
4
6
8
10
12
14
16
18